CMG2004 Abstracts:

(All registered participants as of 11 June, 2004)

Murray	A. Brad	abmurray@duke.edu	60
Nakagawa	Takashi	takashi@geosci.uchicago.edu	61
Neef	Lisa	lisa@atmosp.physics.utoronto.ca	63
Neri	Augusto	neri@pi.ingv.it	64
Neufeld	Jerome	jerome.neufeld@yale.edu	65
Ou	hsien-wang	dou@ldeo.columbia.edu	66
Paldor	Nathan	Nathan.Paldor@huji.ac.il	67
Pasquero	Claudia	claudia@gps.caltech.edu	68
Patra	Abani	abani@eng.buffalo.edu	69
Perez	Cristina	cristina@iri.columbia.edu	70
Perigaud	Claire	cp@pacific.jpl.nasa.gov	71
Robinson	Frank	francis.robinson@yale.edu	72
Rothman	Daniel	dan@segovia.mit.edu	73
Saujani	Simal	simal@atmosp.physics.utoronto.	74
Schertzer	Daniel	Daniel.Schertzer@cereve.enpc.fr	75
Schneider	Edwin	schneide@cola.iges.org	77
Schneider	Tapio	tapio@gps.caltech.edu	78
Scholz	Christopher	scholz@ldeo.columbia.edu	79
Singh	Ramesh	rsingh3@gmu.edu	80
Sobel	Adam	ahs129@columbia.edu	81
Spiegelman	Marc	mspieg@ldeo.columbia.edu	82
Turnewitsch	Robert	rxt@soc.soton.ac.uk	83
Ukita	Jinro	jukita@ldeo.columbia.edu	84
Vyushin	Dmitry	vyushin@atmosp.physics.utoron	85
Waite	Michael	michael.waite@mail.mcgill.ca	86
wells	mathew	mathew.wells@yale.edu	87
Wettlaufer	John	john.wettlaufer@yale.edu	88
Wittman	Matthew	maw2006@columbia.edu	89
Wu	Zhaohua	zhwu@cola.iges.org	91
Wunsch	Carl	cwunsch@mit.edu	92
Yizhaq	Hezi	yiyeh@bgumail.bgu.ac.il	93
Yuen	David	davey@krissy.geo.umn.edu	95
Zaliapin	Ilya	zal@ess.ucla.edu	97
Zaranek	Sarah	Sarah_Zaranek@brown.edu	98
Zhou	Bo	bz81@columbia.edu	100

Two Time-Scales of Pulsation of the Iceland Plume Inferred From Magnetic Anomalies of the North-Atlantic

Meir Abelson[1] (972-2-5314228; meira@mail.gsi.gov.il)

Amotz Agnon[2] (972-2-6584743; amotz@huji.ac.il)

[1] Geological Survey of Israel, 30 Malkhey Yisrael St., Jerusalem 95501, Israel

[2] Institute of Earth Sciences, Hebrew University, Jerusalem 91904, Israel

We have shown previously [Abelson and Agnon, EPSL, 1997, 2001] that small offsets 2nd-order MOR segments, oblique to spreading direction, may indicate a strong influence of a nearby hotspot. We term this anomalous plan-view-geometry of the ridge axis as a planform anomaly (PA). The PA-hypothesis was successfully tested on the ridge-plume system around Iceland, where ancient planforms of the Kolbeinsey Ridge (KR) and the Reykjanes Ridge (RR) are recorded by magnetic anomalies north and south of Iceland, respectively. The magnetic fabric off-KR axis displays variations between normal planform (orthogonal & segmented) and PA in the past 10 Myr. The PA recurrences of the KR correlate with the plume pulses previously inferred by the V-shaped ridges around RR, suggesting that PA records episodes of strong influence of Iceland on KR. Accordingly, the inferred time-scale of cycles of plume pulsation is ~5 Myr. On the other hand, the magnetic fabric around the RR displays variations between normal planform and PA in a time-scale of 30 Myr. The fluctuations between PA and normal planform are made by twist of the 2nd-order segments while preservation of obliquity of the general trend of the ridge on ~30° to spreading direction. From this magnetic record two major pulses of enhanced plume activity are inferred since the formation of the oceanic crust (anomaly #24). The first pulse is between 54 Ma to 39 Ma, compatible with thick igneous crust (18-9 km). The second pulse starts some 20-24 Ma, consistent with the disappearance of off-axis scars (i.e., disappearance of 2nd-order discontinuities along the RR). This long pulse is accompanied with the emergence of the Iceland Plateau. Between the two long pulses, a period of segmented and orthogonal planform suggests a significant decrease of the plume activity between anomalies #17 (38.1-36.6 Ma) to anomaly #6 (20.1-19 Ma), consistent with the deeper seafloor bathymetry. The inference of the PA-pulse linkage and the two time-scales of pulsation may assist in the detection of the plume structure and dynamics. For instance, we suggest that the short-time scale pulsation is due to fluctuations in the flux of plume material, supported by a pinch-and-swell structure of a vertical anomaly of seismic velocity. This structure implies ascent velocity of ~4 cm/y for 5 Myr interval between pulses.

Geologists have recently discerned naturally occurring discrete localized planar zones of deformation, associated with compaction of initially high-porosity rock. Such compaction bands may influence fluid transport, and stress/strain distribution in sedimentary formations. In order to gain insight into the formation mechanisms of compaction bands under a variety of boundary conditions, we developed a discrete model, in which the material is represented as a hexagonal lattice of springs that can transfer only normal forces (Central Force Spring model). The model easily allows for a discrete statistical distribution of material properties at a physically relevant scale. The occurrence of grain crushing and porosity reduction is represented by a change in the equilibrium length and elastic properties of each element that exceeds a certain stress threshold. Parametric analysis is conducted to explore and predict the conditions under which compaction bands form and develop. Some of our results duplicate the different types of compaction propagation observed in laboratory tri-axial compression experiments.

The first part of our work evaluates the role of heterogeneity in material's properties and elastic mismatches at its boundaries due to contact with other materials. Both of these parameters modulate the compaction nucleation sites, and influence the emerging compaction patterns. The second part of our work focuses on the spatial and temporal evolution of a single compaction band nucleated by a small flaw, and discuss how our results compare with the concept of "anticrack" propagation.
Although some of these features have been observed experimentally, our model provides the first quantitative picture of this important physical process.

Adaptable Geophysics Models and Solvers

Bill Appelbe, Steve Quenette, Patrick Sunter
Victorian Partnership for Advanced Computing, Melbourne, Australia

Louis Moresi
Monash University, Melbourne, Australia

Abstract

One key problem that faces geophysics is the high cost of constructing, adapting, and maintaining numerical model s for large scale simulations. Tools such as Matlab or Mathematica can be used to rapidly model and numerically s olve PDEs, but they are not efficient for large scale parallel computations. Libraries such as PETSc and NAG prov ide some adaptability in parallel implicit solvers, but adapting and testing different solvers is still a tedious process that requires recompilation and recoding much of the application. Our work has focused on building a lightweight software framework on top of libraries such as PETSc, NAG, and HYPRE, that supports development of new mod els with minimal recoding or loss of performance. The framework supports both implicit and explicit solvers, and is in use for DNS in geophysics at several sites in the USA and Australia for 2D and 3D CitCom and FLAC style s olvers for visco-elastic flow.

Traditional Code Adaptation

Traditional scientific software is adapted to support new models by one of two means:

1. Cut and paste
   Create a new code that is a copy of the old code with changes such as new solvers or rheology.
2. Modification
   Modify the existing code to incorporate new features (solvers or geophysics). Where an extension is inconsist ent with the existing code, use conditional compilation or conditional statements to choose the appropriate feature set.

Neither of these approaches scale well. Cut and paste can soon create dozens of incompatible versions of a progra m - any change or improvement in one version soon gets out of sync with the other versions of the program. Soon users are faced with a major maintenance problem: different versions of the code are supported on different platfor ms with different quirks and features. By contrast, modification tries to maintain one monolithic version of the app lication. But such monolithic code soon becomes harder and harder to understand and maintain, as the structure of the code is obscured by a thicket of interdependent conditional statements and compilation directives.

In modern systems and business programming, adaptation is provided through OO technology in Java and C++ an d frameworks and plug-ins. A framework is a set of extensible library classes and interface that can be specialized for a particular problem without altering the underlying. A plug-in is an extension that can be added to the framew ork without recompilation of the framework.

Neither Java or C++ and their brand of OO technology have made significant inroads into scientific computing. T he reason is simply that neither language is very efficient for large-scale parallel numerical models and framework s.

The solution to this conundrum is to apply OO style technology (frameworks and plug-ins), but use traditional high -performance C and Fortran programming techniques, make parallelism implicit (in the framework) and build on t op of existing numerical libraries and solvers such as PETSc, NAG, and HYPRE.

The StGermain Framework

The StGermain framework has been developed and evolved over the past three years so that it supports a range of numerical models for lithospheric and mantle flow, using both implicit and explicit solvers and coupled models. T he key abstractions in the framework include support for: grids, meshes, particles, and particle ensembles.

StGermain programs are build around the idea of a Context. A Context has two main roles:
- bringing together all the data structures a program requires, and
- controlling what is run where through a set of EntryPoints.

An EntryPoint is simply a modifiable stack of named function pointers, that can be run on command. An example entry point is outputting visualization information at the end of every solver time step. The combined group of Entr yPoints a program defines forms an API (Applications Programming Interface) that the plugin developer can use to build new numerical models.

StGermain Contexts have three distinct stages:
1. setting up what the application will do, by filling in the entry points with function pointer hooks;
2. allocating memory for data structures and initializing them;
3. doing the real scientific work, by iteratively running the solver.

So how can plugins change how a program runs? The plugin dynamic libraries are loaded at the start of stage 2 abo ve (in Context_Build()), so they can modify the entry points and extend the data structures before the actual main p rogram (solver) runs. Thus, a basic output plugin may simply register a function pointer in the AbstractContext_Du mp entry point. A more complex plugin which adds the ability to model material with a particular rheology may ex tend the particle type with additional information, and modify several key entry points within the solver. Complete flexibility is provided.

The current set of plug-ins include:

Materials: rectangular box initial conditions, slab initial conditions (for subduction)

Solvers: gravity, viscous rheology (the strong temperature dependence of viscosity in mantle convection for Newto nian and non-Newtonian fluids non-dimensional Arrhenius viscosity law, or Frank-Kamenetskii approximation).

Output: boundary layer thickness, iso-surfaces, temperature profiles, surface mobility

Plug-ins also support changing the underlying solver for implicit methods. A key performance issue is often the ch oice of linear solver or preconditioner. The choice of linear solver or preconditioner should almost invariably not b e hard-wired into an application, as any change in the boundary conditions or equations will affect the choice of sol ver. Libraries like PETSc support dynamic choice of solver, and we have extended that to allow link-time binding of solver libraries including PETSc and HYPRE (Algebraic Multi-grid).

The code for StGermain is all open-source, and can be downloaded, along with documentation and demonstration examples from: http://rd01.vpac.org/twiki/bin/view/Stgermain

Presentation

The presentation will discuss the architecture and performance of StGermain for a variety of geophysics applicatio ns, and compare it to traditional monolithic applications such as Terra and CitCom.

WAVE-LIKE PHENOMENA DURING THE MORNING TRANSITION IN THE PLANETARY BOUNDARY LAYER (PBL): A COMPARISON WITH WATER-TANK EXPERIMENTS.

Nicolas Arnault[(1)], Pierre H. Flamant[(1)], Paul Billant[(2)], Jean-Marc Chomaz[(2)]

[(1)]LMD-CNRS, Ecole Polytechnique, 91128 Palaiseau cedex, France, arnault@lmd.polytechnique.fr, flamant@lmd.polytechnique.fr
[(2)]LADHYX-CNRS, Ecole Polytechnique, 91128 Palaiseau cedex, France, billant@ladhyx.polytechnique.fr, chomaz@ladhyx.polytechnique.fr

ABSTRACT

Ground-based LIDAR observations of the morning transition in the PBL have been documented since 2002 and revealed anomalous mixing at the top of the Residual Layer (RL). As an example the case of the 14 October 2003 is presented here. Strong wave-like instabilities appear at the capping inversion of the RL. They seem to be due to convectively-driven internal gravity waves. In order to simplify the overall physics, water tank experiments using shadowgraph technique have been carried out to investigate the generation of internal gravity waves from turbulence in a multi-layered system. These experiments are set to provide a better understanding of the morning transition. Atmospheric thermally driven convection and thermal stratification of the PBL are simulated respectively by mean of mechanical stirring and water-salt stratification. Experiments revealed both transfer of energy by wave propagation and "tunneling-effect" transfer of energy by evanescent waves. Results are compared with observations and analytical model.

1. INTRODUCTION

The Atmospheric Boundary Layer (ABL) plays a major role in air quality problems, with respect to emission, mixing, dilution, transport of gas contaminants and aerosols particles. The RL has a great impact on air quality via down-mixing of pollutants [1]. To our knowledge, only few studies have been devoted to the morning transition. In the morning, RL is generally represented as a neutrally stratified elevated layer, whose characteristics are generally observed to be initially those of the Mixing Layer (ML) from the previous day [2]. However, in some cases, there is evidence of small stratification of the RL which is therefore able to sustain internal gravity wave propagation. Interaction between stratified layers and turbulence generated by an oscillating grid has been studied in various laboratory settings [3-5]. Turbulent forcing at the boundary between turbulent and stratified layers can generate both internal waves and evanescent waves that radiate into the outer stratified layer, carrying energy out of the turbulent layer [6,7]. The present work aim to understand the conditions for the inversion layer above to sustain resonant modes and lead to breaking at the RL height.

2. THE 14 OCTOBER 2003 OBSERVATIONS

An upward looking Elastic Backscatter Lidar (EBL) and a 2µm Heterodyn Doppler Lidar (HDL) have been deployed by the LIMAG Team on the instrumented site of Palaiseau. Zenith lidar observations were performed from 0800 to 1400 UTC. A gradient algorithm has been applied to EBL signal to estimate the RL and ML heights and HDL provides time series of the vertical velocity. The temporal resolution of EBL is 10 s and the spatial resolution is 15 m. The temporal resolution of HDL is 4 s and the spatial resolution is 75 m.

2.1 Wave-like phenomena and mixing at the top of the RL

In Fig.1 EBL time series show the end of the morning transition on the 14 October 2003.

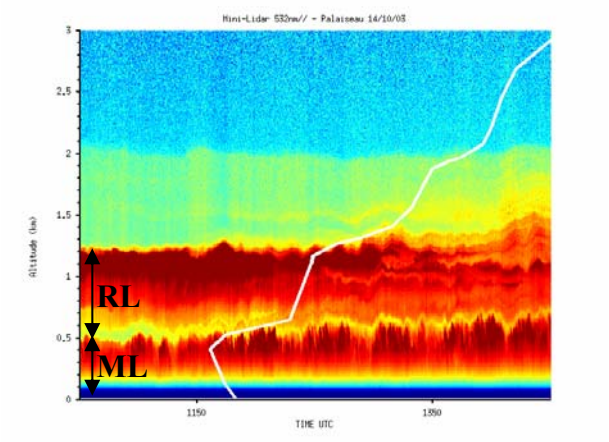

Fig.1 EBL time series of the morning transition on 14 October 2003; Start at 1100 UTC, end at 1400 UTC. The white curve is the potential temperature at 1200 UTC from radio soundings.

The ML reaches 500 m and the RL height is approximately 1200 m. From 1130 UTC to 1320 UTC, waves of amplitude ranging from 50 m to 100 m are clearly visible at the base of the inversion Layer. The wave characteristics i.e. frequency and amplitude can be retrieved from the EBL signal and time series of vertical velocity. After 1320 UTC, mixing occurs at the inversion layer.

3. WATER-TANK EXPERIMENTS

3.1 Experimental set-up

Experiments have been performed in a glass tank of horizontal dimensions W=20 cm, L=42.5 cm and of height H=29 cm. A grid made of small holes of 0.5 cm diameter was used, giving a solidity of 56% even if such solidity is known to generate secondary flow [8]. The tank is filled up to 2 cm from the edge with three layers of uniformly salt-stratified water using the standard double-bucket technique. Each layer is separated from the other by a controlled density jump, assuming small salt diffusion during the experiments. The strength of stratification of each layer is represented by the buoyancy frequency, N, which is defined by

$$N^2 = -\frac{g}{\rho_0}\frac{d\rho}{dz} \qquad (1)$$

where $\rho(z)$ is a background density profile, ρ_0 is a reference density, and g is the gravitational acceleration. The density profiles have been determined by measuring the refraction index of vertical samples of salt water. The grid is oscillated at the top of the tank by mean of a speed-controlled motor. The grid frequency ranges between 0.5 Hz and 1 Hz, with a stroke of 7.3 cm.

The experiments are set to give more insight into the wave generation during the morning transition. A turbulent region created by the oscillating grid is overlaying a weakly-stratified salt-water layer bounded by an inversion and a strongly-stratified layer, modeling respectively the atmospheric convective layer, the near neutral RL and the free troposphere. We have explored a wide range of buoyancy frequency ratio $\varepsilon=N_i/N_u$, where N_i and N_u are respectively the buoyancy frequency of the intermediate layer and the upper layer.

Shadowgraph technique has been used to visualize the turbulent region and the internal wave field. A light source illuminates the water-tank and a white screen is placed behind the tank. A CCD camera is positioned perpendicularly to the front of the tank. 4 Hz acquisitions of the flow are made. The sharp density jumps allow us to visualize clearly the interfaces between the layers.

3.2 Qualitative observations

Fig.2 shows the instantaneous flow. The z axis has been turn upside-down in order to be similar to the atmospheric case. The wave-field has been enhanced by subtracting the image to a reference image. The lower part is the turbulent region generated by the oscillating grid, with a clear turbulent front. The mid-line is the interface between the two layers of stratified fluids. Waves are clearly visible in the upper and intermediate layers as shown by dark and light oblique regions. Characteristics directions of the wave's propagation are also visible, which allow us to estimate the wave frequency in both layers, using the dispersion relation for internal gravity waves

$$\omega = N\cos\theta \qquad (2)$$

where ω is the wave frequency (rad.s^{-1}), N the buoyancy frequency (rad.s^{-1}) and θ the angle of the wave number with respect to the vertical. This experiment reveals upward propagation of internal gravity waves in the intermediate layer which is weakly stratified. Part of the wave energy is converted into interface displacement which in turn propagates upward internal gravity waves in the strongly-stratified layer above.

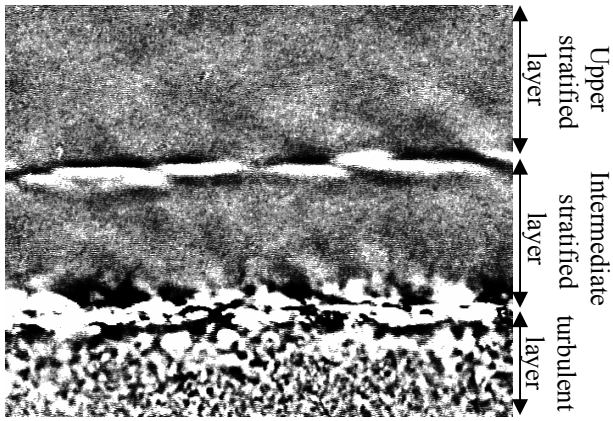

Fig.2 Upward internal gravity waves in a three layer system.

3.3 Quantitative results

A detection algorithm has been used to provide time series of the relative displacement of the interface between the two stratified layers. The length of the interface detection is approximately 18 cm. Time series of 1min are recorded at a sampling frequency of 4 Hz, enabling a spectral analysis. Fig. 3 shows the frequency spectrum of the time series. This spectrum is divided into three main regions corresponding to different physical behaviors. The first region below N_i is related to propagation of internal gravity waves in the intermediate layer. The second region lies between N_i

and N_u and corresponds to the transfer of evanescent waves through the intermediate layer. This region and the peak located near N_u are due to what we referred as a "tunneling effect" transfer of energy. The third region is located around the grid frequency f_g and is related to the secondary flow generated by the grid.

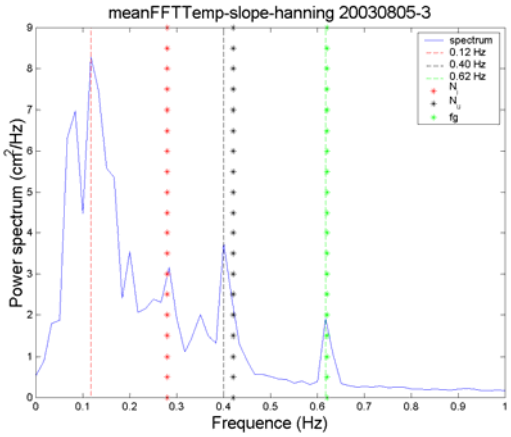

Fig.3 Power spectrum of the time series. Main peak frequencies are dashed lines. Red dotted line is N_i, black dotted line is N_u and green dotted line is the grid frequency f_g.

4. REFERENCES

1. Fochesatto, G. J., and Drobinski, P., et al. *Evidence of dynamical coupling between the residual layer and the developing convective boundary layer*, Boundary-layer Meteorol. 99, 451-464, 2001.
2. Stull, R. B., *An introduction to boundary layer meteorology*, Kluwer Academic Publishers, Dordrecht, 666 pp.
3. Linden, P. F., *The deepening of a mixed layer in a stratified fluid*, J. Fluid Mech. 71, 385, 1975.
4. E, X., and Hopfinger, E. J., *On mixing across an interface in stably stratified fluid*, J. Fluid Mech. 166, 227, 1986.
5. Dohan, K., and Sutherland, B. R., *Internal waves generated from a turbulent mixed region*, Phys. Fluids 15, 488-498, 2003.
6. Perera, M. J. A. M., Fernando, H.J.S., and Boyer, D. L., *Turbulent mixing at an inversion layer*, J. Fluid Mech. 267, 275-298, 1994.
7. Stull, R. B., *Internal gravity waves generated by penetrative convection*, J. Atmos. Sci. 33, 1279-1286, 1976.
8. De Silva, I. P. D., and Fernando, H. J. S., *Some aspects of mixing in a stratified turbulent patch*, J. Fluid Mech. 240, 601-625, 1992.

A particle sedimentation model of buoyant jets based on observations of hydrothermal plumes

Karen G. Bemis, Deborah Silver, Peter Rona
Rutgers University

The input for standard models of buoyant jets (whether volcanic or hydrothermal in origin) only specifies volume flux and particle concentration at the vent. This is appropriate for volcanic eruption plumes, where any information is likely to be localized at the vent. However, in seafloor hydrothermal systems, the particle concentrations within the plume are more easily measured than estimates of input particle flux based on chemical concentrations and predictions (there are no particles in the exiting fluids; they precipitate after the vent fluid mix with seawater). Thus, we are developing a particle sedimentation model that uses observed velocity and particle distributions in plumes (from remote sensing acoustic images of hydrothermal plumes) as input. As satellite observation of volcanic clouds become more sophisticated this may have broader applicability.

A generalized law for aftershock rates in a damage rheology model

Yehuda Ben-Zion (1) and Vladimir Lyakhovsky (2)

(1) Department of Earth Sciences, University of Southern California Los Angeles, CA, 90089-0740, USA; e-mail: benzion@usc.edu; phone: 1-213-740-6734; fax 1-213-740-8801
(2) The Geological Survey of Israel, Jerusalem, Israel; e-mail: vladi@geos.gsi.gov.il

Aftershocks are the response of a damaged rock surrounding large earthquake ruptures to stress perturbations produced by the large events. Lyakhovsky et al. [JGR, 1997] developed a damage rheology model that provides a quantitative treatment for macroscopic effects of evolving distributed cracking with local density represented by a state variable α. The equation for damage evolution, based on thermodynamics of energy balance and entropy production, and generalization of Hookean elasticity to irreversible brittle deformation, accounts for degradation and healing as a function of the strain tensor and material properties (rate coefficients and ratio of strain invariants separating states of degradation and healing) that may be constrained by lab data. Analyses of stress-strain and acoustic emission laboratory data during deformation leading to brittle failure indicate further [Hamiel et al., GJI, 2004] that the fit between model predictions and observations improves if we also incorporate gradual accumulation of a non-reversible deformation with a rate proportional to the rate of damage increase.

For analysis of aftershocks, we consider the relaxation process of a material following the application of a strain step associated with the occurrence of a mainshock. The coupled differential equations governing the damage evolution and stress relaxation can be written in non-dimensional form by scaling the elastic stress to its initial value and the time to characteristic time of damage evolution τ_d. With this, the system behavior is controlled by a single non-dimensional ratio $R = \tau_d/\tau_M$ representing the ratio between the damage time scale to the Maxwell relaxation time τ_M. For very small R there is no relaxation and the response consists of constant rate of damage increase until failure. For very large R there is rapid relaxation without significant change to the level of damage. For intermediate cases the equations are strongly coupled and nonlinear. The analytical solution for the damage evolution contains error functions and is richer than a simple power law relation. However, the results associated with the analytical expression can be fitted well for various values of R with a power law similar to the modified Omori law for aftershocks. This also holds for 3D numerical simulations of aftershock sequences with our damage rheology model. Initial results based on 3D simulations indicate that high values of R corresponding to low viscosity material produce diffuse (swarm-like) aftershock sequences, while low values of R corresponding to more brittle material produce clear (Omori-like) aftershock sequences.

Rossby wave interaction connecting the tropics and midlatitudes: a new asymptotic theory and solitary waves

Joseph A. Biello with A.J. Majda

Abstract

Equatorial baroclinic Rossby waves are equatorially trapped and can respond to equatorial diabatic heating. Equatorial barotropic Rossby waves have a significant projection and midlatitudes. Both of these families of Rossby waves are weakly dispersive in the limit of long zonal wavelength and their wave speeds allow for resonant interactions on intraseasonal timescales. We have developed simplified asymptotic equations for the nonlinear interaction of long wavelength equatorial Rossby waves and barotropic Rossby waves with a significant midlatitude projection in the presence of suitable horizontally and vertically sheared zonal mean flows. The simplified equations allow for nonlinear energy exchange between the barotropic Rossby waves and the baroclinic equatorial waves for non-zero zonal mean vertical shear through wave-wave interactions. Idealized examples in the model demonstrate that midlatitude Rossby wave trains in a baroclinic mean shear can transfer their energy to localized equatorially trapped baroclinic Rossby waves through a nonlinear "westerly wind burst" mechanism. Conversely, equatorially trapped baroclinic Rossby wave trains in the idealized model can transfer substantial energy to the midlatitude barotropic Rossby waves. From the viewpoint of applied mathematics, the asymptotic equations derived here have several novel features. In particular, they admit analytic solitary wave solutions which correspond to interesting localized vortical flows in the equatorial troposphere.

Two-dimensionalisation of rapidly rotating turbulence

Lydia Bourouiba and Peter Bartello, McGill University

Over the last decade renewed interest in rapidly rotating turbulence has led to a number of studies employing numerical simulations, laboratory experiments and asymptotic analysis. The point of departure for much of this work has been the Taylor-Proudmann theorem. This classical result merely states that if a rapidly rotating flow evolves slowly with respect to the inverse Coriolis parameter (in other words if the Rossby number, Ro, is small), then the flow must be at least close to two-dimensional. It says nothing about how such a state is achieved starting from, say, isotropic initial conditions.

In problems involving fast waves and slow vortical motions, the important nonlinear interactions are the resonant ones. Only these interactions drive a particular mode's amplitude on the slow timescale. Using this fact and an "instability hypothesis", Waleffe (1993) argued that the nonlinear transfer in rotating turbulence is preferentially towards smaller, but non-zero, $|k_z|$. However, since resonant interactions between a 2D mode ($k_z = 0$) and two inertial wave modes (with $k_z \neq 0$) have a vanishing coupling coefficient, a decoupling of the slow 2D modes from other degrees of freedom is predicted in this limit. Early simulations of decaying rotating turbulence starting from isotropic initial conditions (Bartello, Metais and Lesieur JFM 1994) showed a more rapid decrease of the energy contribution from wave modes than from slow modes. The resulting quasi-2D flow emerged via a more efficient downscale cascade of 3D (or wave) energy. Later, Mahalov et al (1997 Theor. Comput. Fluid Dyn.) predicted not only a decoupling of slow 2D vortical modes from wave modes, but in addition a freezing of the nonlinear transfer at all vertical wavenumbers. This was due to the emergence of an infinite set of adiabatic invariants in the limiting equations at infinite rotations. Recently Cambon, Rubinstein and Godeferd (NJP 2004) have argued that previous work has ignored a wave-vortex interaction that remains active even at large rotation rates, provided the geometry of the flow permits it. This analysis is also not valid if $k_z = 0$.

In this study we use direct numerical simulation to study the mechanism of two-dimensionalisation in inviscid and decaying rotating turbulence. In addition, we perform simulations starting from a quasi 2D state, observing the generation of three-dimensional inertial wave motion, as well as simulations in which there is no initial energy in two dimensional modes. The inviscid truncated model is compared with equilibrium statistical mechanics and decaying simulations were also performed. The resulting behaviour supports the decoupling of the two in the asymptotic limit. However, the Rossby number scaling is quantified and the inhibition of vertical transfer of wave energy will be reported on.

Recent forced simulations of rotating turbulence by Smith and Waleffe (Phys. Fluids 1999) and Chen et al (unpublished 2004) have shown an upscale cascade of quasi 2D motion. These results are interpreted in light of the present study.

The Baikal Rift region is geologically complicated. The rift, an archean craton, and 6 km of sediment in the Baikal Lake influence seismic paths. This structure requires modeling of seismic waveforms that will focus on finding an optimal solution efficiently.

The standard approach to seismic waveform modeling is using a grid search. This method is at best cumbersome, which produces a broad solution set. At its worst a grid search is an impossible task that would take years to perfor m.

An improvement to the grid search approach is simulated annealing. This method perturbs an initial model, searchi ng for better models but allows other models to be accepted with a decreasing probability. This allows the choice o f models to move out of local minimums to find the global minimum.

This technique works if there is a clear global minimum but with complicated structure, as in the Lake Baikal regio n, simulated annealing has no guarantee of finding a global minimum. Multiple objective optimization takes a diffe rent angle perturbing a solution, accepting a less accurate model that is close to a set of dominant models based on the parameters to be minimized. This prevents the solution from diverging from the best solutions and performing unnecessary calculations making this technique more efficient.

CMG2004: 25th IUGG Conference on Mathematical Geophysics
==========

Samuel Burns
Poster

Title:
The Sensivity of a Moist Model of the Hadley Circulation
to Varying the Surface Latent Heat Flux.

Abstract:
The goal of this study is to determine the nature of the
feedback between the surface latent heat flux and the
strength and width of a moist axisymmetric (Hadley) circulation.

The Quasi-Equilibrium Tropical Circulation Model (QTCM) (Neelin and Zeng, 2000)
is solved for an aquaplanet domain with a zonally
symmetric equatorial SST distribution and globally uniform
insolation. The QTCM calculates moisture explicitly, has a
Betts-Miller type convection scheme, and projects the vertical
structure of atmospheric variables on a set of basis functions
(one each for temperature and moisture, and two for momentum) that
are designed to optimize the model's representation of
tropical convection.

The QTCM exploits the idea of statistical
quasi-equilibrium, in which the factors that influence small scale convection
are assumed to be in near equilibrium on the timescale of the large scale
dynamics. This assumption allows the the equations of motion and the complexity
of the model to be simplified while still producing realistic atmospheric
circulations.

Two experiments are performed varying the exchange coefficient in the bulk
formula for the surface latent heat flux, one with a
fixed SST lower boundary condition and another with a
slab mixed layer ocean with a parameterized Q-flux.
In both cases it is shown that the circulation is found to be
strongly dependent on the exchange coefficient, indicating that
surface flux feedbacks are important in determining
the simulated circulation.

Biogeochemical susceptibility of ancient oceans to extreme isotopic events

Alison M. Cohen and Daniel H. Rothman, M.I.T.

It has been suggested that Precambrian oceans (before 543 milion years ago) contained a pool of dissolved and sus pended organic carbon which was significantly more concentrated than the modern ocean. This high concentration is traced to its accumulation in the water column, prior to the evolutionary innovations that caused organic matter t o sink. Oxidation of a small part of this large reservoir can create a large isotopic signal in the smaller inorganic p ool, thereby explaining the large fluctuations of isotopic composition of carbonate in the late Precambrian geologic record. Here we construct a simple continuous model to analyze the mechanisms by which such an organic-rich o cean can be created and investigate its stability with respect to oceanic circulation and evolutionary changes. Our model describes the biological, geochemical, and physical interactions of oceanic organic carbon, dissolved oxyge n, and dissolved inorganic nutrients as a function of depth. It is formulated as coupled advection-reaction-diffusio n equations. We first verify that, in the presence of sinking organic matter, the model simulates modern depth prof iles of oxygen, carbon, and nutrients such as phosphorus. We then explore the consequences of producing neutrall y-buoyant organic matter.

First-principles Multiscale Modeling of Earth Materials Properties

Ronald Cohen
Geophysical Laboratory
Carnegie Institution of Washington

A long-term goal of computational mineral physics in particular, and theoretical materials research in general, is to be able to predict properties of complex materials, and predict phase diagrams and dynamical processes, without resource to experimental data, and with accuracy rivaling or surpassing that of experimental studies. First-principles computations of many materials properties for pure perfect ordered compounds at zero temperature within the local density approximation (LDA) of density functional theory (DFT) are now straightforward, although still interesting and computationally intensive. The predictive accuracy of these current methods is generally well known, but varies with the material chemistry. Volumes for example, tend to be within a few percent of experiment, and elastic constants within 10-20% for ionic transition element free materials. The frontier areas are (1) developing more accurate DFT methods, (2) obtaining thermal properties, and (3) modeling solid solutions and disordered materials such as liquids. Active areas in developing DFT are moving beyond the LDA and generalized gradient approximations (GGA), which are accurate for many systems, but problematic in others. Included in these developments are new general methods, and methods that are specific to particular classes of materials, such as LDA+U and dynamical mean field theory (DMFT) for transition metal ion materials, such as ferrous iron in minerals. Thermal properties can be obtained from classical molecular dynamics on very short time scales for small systems using self-consistent electronic structure methods, or various statistical mechanical approximations such as quasiharmonic lattice dynamics or the particle in a cell method. In order to obtain properties for complex solid solutions or complex rheological or time-dependent properties, a multiscale approach is necessary, where results from smaller length/time scales are used to constrain models at a larger length/time scale. Applications of such an approach to ferroelectrics and magnetism in iron will be shown.

FLOW INSTABILITIES INDUCED BY VISCOUS HEATING IN MAGMA CONDUITS

A. Costa and G. Macedonio
Osservatorio Vesuviano-INGV, Via Diocleziano 328, Napoli, Italy.

Silicate melt viscosities show a strong dependence with temperature. Temperature-sensitivity of magma viscosity implies a relevant coupling between the energy and momentum equations. The heat generated by viscous friction produces a local temperature increase near the tube walls with a consequent decrease of the viscosity and a strong stratification in the viscosity profile .
The temperature rise due to the viscous heating may trigger instabilities and secondary flows in the velocity field which cannot be predicted by a simple isothermal Newtonian model. This kind of instabilities are similar to those observed in core-annular flows of two fluids with different viscosities with the less viscous fluid near the tube wall.
Using a direct numerical simulation, here we show, how in certain regimes, these effects can trigger and sustain a particular class of secondary rotational flows which appear organised in coherent structures similar to roller vortices.

Development of perturbations on a buoyant coastal current

Olof H Dahl
Department of Oceanography, Göteborg University,
Göteborg, Sweden (olda@oce.gu.se).

The dynamics of a small perturbation on a coastal current in a buoyant upper layer of the ocean is investigated. The active upper layer vanishes at a certain distance away from the coast, forming a front. The perturbations are imposed on a steady basic state with no along-coast variation. Analytical solutions are derived for two special configurations of the background state: (i) constant along-shore velocity, i.e. a coastal current with triangular cross-section and (ii) a constant potential vorticity current. In both cases we find two wave modes: a slowly moving frontally trapped wave, and a coastally trapped wave that moves approximately with the internal Kelvin wave speed plus the current speed at the coast. These two wave modes are not sufficient to build up a generally shaped initial perturbation. The part of the initial perturbation not covered by the two wave modes will in case (i) split into an infinite number of higher wave modes all travelling faster than the frontal wave and in case (ii) be advected and slowly smeared out by the current. We find that for all physically relevant cases the perturbations always move in the direction of the Kelvin wave, ie., in the same direction as the coastal current, as long as the current is unidirectional.

WAVELET EVALUATION OF INVERSE VENING MEINESZ INTEGRAL

Neda Darbeheshti
Darbeheshti@ncc.neda.net.ir

Abstract

Nowadays wavelet transform is a powerful tool in numerical analysis. Wavelet expansions and wavelet transforms have proven to be very efficient and effective in analyzing a very wide class of signals and phenomena, Because (a) they have localization properties in both the time (space) and frequency (scale) domains and (b) the generation of wavelets and the calculation of the discrete wavelet transform is well matched to the digital computer.

Numerical calculation of some integrals such as Stokes integral has been important in geodesy and geophysics. In this paper the numerical solution of Inverse Vening Meinesz integral using wavelet transform has been done and the wavelet method is compared with point wise integration and Fast Fourier Transform in terms of computational efficiency and accuracy.

Inverse Vening Meinesz integral transforms deflections of vertical to gravity anomalies. Here deflections of vertical have been provided by satellite altimetry technique over the Oman Sea.

FRACTAL DIMENSION OF MEASURING NETWORK: IMPLICATIONS IN INTERPOLATION AND DETECTIBILITY

V.P. Dimri, Ravi P. Srivastava and Nimisha Vedanti

National Geophysical Research Institute, Hyderabad, 500 007, India

Spatial locations of many geophysical data sets are inhomogeneously distributed. Gridding of such data suffers from the interpolation errors which are manifested in terms of spurious anomalies due to aliased interpolated data. Short wavelength anomalies of potential field data produce aliasing, which can be minimized using fractal analysis. There are many techniques for characterization of data distribution viz. Nearest Neighbours Index, Morisita Index, Thiessen/ Voronoi polygons and Coefficient of Representativity. The fractal dimension of measuring network characterizes the data distribution and represents the density of data distribution in simplest way unlike other mentioned techniques. Using fractal dimension optimum gridding interval can be obtained which is used for optimum interpolation interval obeying Shanon's sampling theorem. The optimum interpolation interval is the shortest length at which the scaling regime is constant. The technique is applied on a few synthetic data distributions and on a real gravity/magnetic data set collected in Vindhyan basin, India. The fractal dimension of the measuring network is determined using box-counting method and the detectibility limit of the source distribution has been obtained for the real data of Vindhyan basin[1]. A fractal dimension of recently obtained data set in Vindhyan basin is found to be 1.68, leading to detectibility limit of 0.32. Thus sources with fractal dimension less than 0.32 can not be detected with the said measuring network.

Keywords: fractal dimension, detectibility limit, interpolation

References

[1] **V.P. Dimri,** 1998, Fractal behavior and detectibility limits of geophysical surveys, Geophysics, 63, 1943-1947.

A pair of chaotic dynamical systems can synchronize when loosely coupled in a variety of ways. It is suggested that the synchronization phenomenon, with one system representing "truth" and the other system representing "model," provides a new approach to data assimilation in high-dimensional systems, reminiscent of Carl Jung's notion of synchronicity between matter and mind. One is led to search for low-dimensional subspaces through which the two systems can be synchronously coupled, such as a subspace defined by a small number of local bred vectors. Using a pair of 2-layer quasigeostrophic channel models, the efficacy of a bred vector basis for data assimilation can thus be compared to that of other bases.

It is argued that the synchronization approach differs qualitatively from any of the standard approaches to data assimilation. An equation for synchronously coupled dynamical systems can be obtained for continuous data assimilation in a linearized model, with coupling strength given in terms of observation and background errors in the usual way, and with observation error taken to correspond to noise in the coupling channel. Background error is computed from an assumption of stationarity of the probability distribution function (PDF) that satisfies the corresponding Fokker-Planck equation, for the case of a perfect model. An optimal coupling, in contrast, can be defined as one that minimizes the spread of the PDF. The analysis is used to motivate a suggestion that the synchronization approach to computing the optimal coupling for the full nonlinear model will improve upon more empirical methods.

Towards Limnological Modeling of the Dead Sea: Mass and Heat Balances

Dvorkin Y., Lensky N., Lyahovsky V., Gavrieli I
Geological Survey of Israel, Malkhei Yisrael St. 30, 95501 Jerusalem, Israel

The Dead Sea (DS), the lowest place on Earth, is a hypersaline terminal lake with a unique composition. During the 20th century, the DS level has dropped by more than 20 meters, and presently it is about 417 meters below mean sea level. The decline in the DS level is a manifestation of the negative water balance of the lake, whereby evaporation greatly exceeds inflow. This is due to diversion of freshwater from the catchment area of the DS and results in the collapse of the infrastructure around the lake. The rate of water level drop over the last few years is more than 1 m/yr, which translates to an annual water deficit of about 625 million cubic meters. Yet, the total water balance of the DS is still controversial since the subsurface inflows and rate of evaporation are not directly measurable. To make up for this water deficit, a channel connecting the DS with the Red Sea is considered ("Peace Conduit"). To judge the feasibility of such a project, it is necessary to understand its long-range impact on the evolution of the DS. It is essential that these man-made changes will not result in environmental and economical damages that will surpass the present damages. Furthermore, the limnological behavior of the new DS-seawater system must be modeled in order to minimize damages and to correctly engineer the conduit in terms of volume, mode of introduction of seawater and timing of inflow.

Mixing of seawater or concentrated seawater after desalinization (density up to 1,060 kg/m^3) with original DS brine (density above 1,240 kg/m^3) is expected to result in stratification of the water column with a mixed layer of DS-seawater and concentrated DS brine as the lower water body, as well as continuous change in the brine composition. The density difference between DS brine and seawater exceeds 20% and the mixing process is not volume-conservative due to chemical interaction. Thus, the modeling of the turbulent mixing, vertical and horizontal brine circulation, and temperature distribution within the basin of the DS should be non-Boussinesq and account for water compressibility. Most of existing limnological/oceanographic models use Boussinesq approximation ignoring the water compressibility and should be significantly modified to meet the DS conditions. Additional complication arises from the halite (NaCl) precipitation as a result of the evaporation from the surface and precipitation of gypsum and other minerals as a result of DS-seawater mixing.

Currently we are developing 1-, 2- and 3-D models for the DS. Here we present a framework for the calculations of subsurface inflow and rate of evaporation using energy and mass balance considerations. Overall heat balance calculations were conducted by separate calculations of the several heat budget terms. The only measured term in the heat balance is short wave solar net radiation. All other terms were calculated using measured sea surface and air temperatures and relative humidity. The calculated heat

budget terms include long wave net atmospheric radiation, back radiation from the water surface, evaporative heat flux and conductive heat flux. The mass of evaporated water and mass of precipitated salts were calculated from the energy considerations and change in salinity. This, along with known annual water deficit, surface inflows and measured overall heating of the DS water body provide constraints on the subsurface inflows.

Another aspect studied was the differences between the volumes of water evaporated vs. the change in the volume of the lake. Our calculations show that, without inflows, outflows and salt precipitation the volume change in the DS is about 2% smaller than the volume of evaporated water.

We modified the 1-D Princeton Oceanographic Model (POM) incorporating the new equation of state. Following the Mellor and Yamada [1982] turbulent closure scheme, vertical mixing is simulated by turbulent diffusion with coefficient depending on the Richardson number. Since the horizontal velocities can not be properly calculated in a 1-D model, we assume exponential decay of the kinetic energy with depth according to the Ekman layer considerations. 1-D model was calibrated using meteorological data and water level measurements. The model correctly reproduces the measured temperature and salinity profiles, sea level drop and seasonal stratification and overturn of the DS. The presented modeling allows reducing the uncertainty of the underground inflows and amount of evaporated water.

In the future work, after fully calibrating non- Boussinesq, compressible versions of 2-D (W2-QUAL, Cole and Wells, 2001) and 3-D (POM, Z-grid, Blumberg and Mellor, 1987) models we will model the introduction of seawater into the DS in order to determine the depth of stratification and the change as a function of time in the composition and salinity of the surface water.

REFERENCES:

Blumberg, A. F., and G. L. Mellor, 1987: A description of a three-dimensional coastal ocean circulation model. In: N. Heaps (Ed.), *Three-Dimensional Coastal Ocean Models,* pp 1-16. American Geophysical Union, Washington, DC.

Cole, T. and S. A. Wells, (2001) “CE-QUAL -W2: A Two-Dimensional, Laterally Averaged, Hydrodynamic and Water Quality Model, Version 3.1, ”Instruction Report EL -2001-, USA Engineering and Research Development Center, Waterways Experiment Station, Vicksburg, MS.

Mellor, G. L., and T. Yamada, 1982: Development of a turbulence closure model for geophysical fluid problems. *Rev. Geophys. Space Phys*. **20**, 871-875.

Implications of self-modulated WWBs on ENSO variability

Ian Eisenman and Eli Tziperman

While the oscillatory tendency of ENSO (El Nino - Southern Oscillation) may be fairly well understood today, debate exists about the relative importance of two popular mechanisms to explain the irregularity. The first is deterministic chaos within the interannually varying components of the coupled ocean-atmosphere system and the second is noise from uncoupled weather forcing. The component of this weather noise that is most important to ENSO variability is believed to be westerly wind bursts (WWBs), which can trigger El Nino events. Recent indications suggest that WWBs may be more prone to occur during certain configurations of the SST, thus controlled to some extent by ENSO. We have investigated the dynamical implications of internally modulated WWBs on ENSO stability and irregularity by examining the extreme case of WWBs that are completely determined by the SST, and thus part of the internal ENSO dynamics, in an intermediate complexity ENSO model.

We find that if WWBs are modulated by the SST, the inclusion of this coupling in stochastically forced models may be crucially important. When the deterministic WWB trigger is replaced in our linearly stable model with a purely stochastic trigger, ENSO variability is reduced by a factor of nearly two.

Results of this work also show that in terms of ENSO stability and irregularity, a strong analogy can be drawn between the occurrence of internally regulated WWBs and the enhancement of the ocean-atmosphere coupling strength. This implies that if WWBs are indeed modulated by the SST, the deterministic chaos and weather forcing mechanisms for ENSO irregularity may be largely equivalent.

Identification of Mantle plumes using Second Generation Wavelets

Gordon Erlebacher, David A. Yuen, and Oleg V. Vasilyev

Mantle convection is a strongly time-dependent processe and has many different scales. Identifying plumes at high Rayleigh numbers and computing their quantitative properties, such as their width and the local heat-flow within them, is an outstanding problem. Automating this process in a reliable manner will help process the increasingly large time-dependent datasets that result from many numerical simulations, needed because of the vast parameter space. Applications of plume identification include computing and constraining the heat budget of the core-mantle boundary, the birthplace of plumes, and computing various heat contributions from various sources, such as viscous heating. Unless the plumes are identified reliably, auxiliary computations will include other contributions from the adjacent mantle outside the plumes, which will skew the results.

One difficulty in reliable plume identification emerges from the continuous nature of the variable (usually temperature, but also composition or both) used to characterize the plumes. Thermal and Thermal-chemical fields have no distinct boundary (i.e., constant temperature, constant temperature gradient, constant composition or a mixture of both). When considering mantle convection in a heated-from below configuration, plumes are usually considered to be regions where the horizontal gradient, or gradients in the case of thermal-chemical convection, is locally stronger than outside the plume. This criterion if of course too simplistic since at high Rayleigh numbers, false plume identification is likely from the strong temperature fluctuations, or from the thinner thinner still chemical fluctuations. Thus far there have been very few studies exist with the intent of identifying plumes; one such uses pattern-recognition techniques (Labrosse 2002).

We use second generation wavelets as a means to identify these plumes (Erlebacher *et al.* 2002). Second generation wavelets are a multiscale technique, which are a generalization of the original wavelets formulations (Sweldens 1997), which compute a wavelet basis by scaling and translating a single mother wavelet. Rather, second generation wavelets transform physical data into a wavelet basis solely through in-place transformations in physical space. This is particularly useful for large datasets. Furthermore, it is possible to establish a one to one correspondance between wavelet coefficients and positions in physical space. Wavelets allow the simultaneous analysis of frequency and spatial structure. Thus, it should be possible to better characterize the structure of plumes: large and small scale components can be distinguished, and selectively retained or removed. The frequency content at both scales can be controlled independently.

To identify the scales of relevance in a plume, we considered the temperature field, which nicely characterizes upwelling and downwelling plumes. After transformation to wavelet space, we performed a hard thresholding operation, which sets to zero all wavelet coefficients whose magnitude falls below a a user-set value. This effectively removes all low and high frequency components that do not contribute significant "energy" to the temperature. The structure location is identified by plotting the positions of the wavelet coefficients in physical space, shown in the bottom three panels of Figure 1. From left to right, we show the strongest 0.8%, 1.2% and 6% of the wavelets. It is clear that the plumes are well captured. The top three panels shown a volumetric reconstruction of the temperature field after performing an inverse wavelet transform (having performed the thresholding operation).

Figure 2 shows the temperature field one plane away from the cold plate (the dataset is 97^3 with $Ra = 10^6$. The wavelet coefficients that exceed a fixed threshold are plotted as black squares. The figure illustrates clearly that the thin, cold filaments are well captured by the wavelet coefficients.

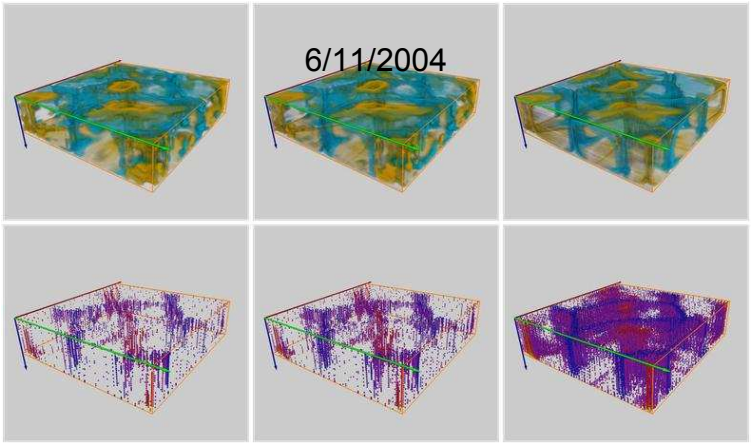

Figure 1: Wavelet coefficients (top) and volumetric reconstruction (bottom) of the temperature field. Left: 0.8%, middle: (1.2%), right: (6%) of the wavelet coefficients are retained during thresholding.

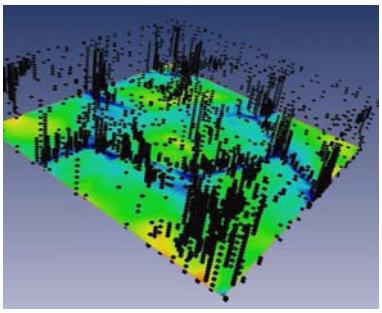

Figure 2: Temperature field in a plane with the positions of the wavelet coefficients of strongest magnitude.

We will discuss our approaches to plume identification, data compression, and heat flux computation within the plumes. Pitfalls, and issues will be detailed. In addition, we will describe some preliminary results in which we use discontinuous second generation wavelets to detect phase diagrams in systems with two degrees of freedom.

Additional work is necessary to determine appropriate values for the threshold, and perhaps identify better variables with stronger correlations to whatever geoscientists consider to be a plume, whether it be thermal or thermal-chemical. To some degree, plume identification is akin to coherent vortex identification in fluid turbulence. Despite several decades of research, scientists have not yet converged on a single working definition.

References

Labrosse, S., Hotspots, mantle plumes and core heat loss, Earth Planet. Sci. Lett., 199, 147-156, 2002.

W. Sweldens. The lifting scheme: A construction of second generation wavelets. SIAM J. Math. Anal., 29:511526, 1997.

G. Erlebacher, D.A. Yuen, F. Dubuffet, Case Study: Visualization and Analysis of High Rayleigh Number – 3D Convection in the Earth's Mantle, *IEEE Visualization '2002/*, pp. 529–532, (October 2002).

Pacific decadal variability in the view of linear equatorial wave theory

Julien Emile-Geay and Mark Cane

May 10, 2004

Abstract

In attempts to better understand the roles of the various components of the Tropical ocean circulation in a "$V'\bar{T}$ mechanism" of decadal variability [*McPhaden and Zhang*, 2002] , we have used a simple model of the Tropical Pacific sea-surface temperatures, with linear, wind-forced dynamics and non-linear thermodynamics. It is shown that decadal wind-forcing alone is able to generate temperature fluctuation of about $0.25°$ C in the Eastern Equatorial Pacific (i.e. on the same order of magnitude as the 76/77 shift), without the need for any atmospheric retroaction. Contrary to the proposed mechanisms cited above, we find that the dominant terms in this budget are :

- the mean upwelling of subsurface temperatures anomalies associated with the thermocline motions
- zonal advection acting upon the large zonal SST gradients.

The anomalous meridional convergence is one of the smallest in the heat budget when considered acting directly upon the mean temperature gradient (the $V'\bar{T}$ term). However, it is crucial to the existence of thermocline depth anomalies, hence to subsurface temperature anomalies, by way of mass conservation.

Consequences of adiabatic decompression melting on magmatic channeling instabilities

Yanming Fang and Marc Spiegelman
Dept. of Applied Physics and Applied Mathematics
Columbia University
yf91@columbia.edu

In the partially molten region of the earth, the solid mantle upwells and melts due to adiabatic change in pressure. The melts that are produced, however, can react with the upwelling solid to form dissolution "channels" which may have widths of 0.1-100 m or larger. A lot of work has been done to understand this process for the problem of a static solid being fluxed by a reactive melt. However, it is still unclear how the solid upwelling affects the channel formation process. A 1-D column model is used to explain the process for the upwelling reactive system. Based on the original nonlinear equations governing flow in reactive, deformable media, we now include the effect of solid upwelling velocity in a simplified linear model. Linear analysis shows that there exists a critical value of both the upwelling velocity and the reactive region height, beyond which no channels can be observed in the reactive region. A phase diagram of the existing channels is generated from the linear analysis and we combined the model with the observational information about the earth to verify the existence of channels in the partially molten region. Both the linear analysis and the numerical model supports the result that channels could exist in the earth yet is affected by different value of solid upwellings and region height.

The major bends of the San Andreas fault (SAF) in California are associated with significant variations in the along-fault topography. We demonstrate that the topography-induced perturbations in the intermediate (vertical) principal stress may enhance bending of a non-optimally oriented fault due to a rotation of the direction of the maximum shear stress in the brittle crust. The shear stress is predicted to rotate away from the maximum compression axis provided that the fault is non-vertical, the long-term fault slip is horizontal, and the fault geometry tends to evolve to a state that dissipates the least amount of the mechanical energy. The observed rotation of the fault plane due to variations in topography along the SAF is used to infer the magnitude of the in situ differential stress. Our results suggest that the average differential stress in the upper crust is of the order of 50 MPa, implying that the effective strength of the San Andreas fault is about a factor of two less compared to predictions based on the Byerlee's law and the assumption of hydrostatic pore pressures, but is on the high end of of constraints provided by the heat flow measurements.

Dynamically adaptive geophysical fluid dynamics simulation using GASpAR

Duane Rosenberg, Aimé Fournier* & Annick Pouquet
Geophysical Turbulence Program, National Center for Atmospheric Research,
PO Box 3000, Boulder, Colorado 80307-3000

Adaptive methods for numerically solving PDEs are now being offered by the numerical-methods and associated communities more frequently, are improving in quality and are being applied to a growing number of science applications. At the same time, turbulent-flow problems continue to be prominent in many geoscience areas e.g., meteorology, oceanography, climatology, ecology and solar-terrestrial interactions. Due to the inherent spatio-temporal complexity of such flows, adaptive methods have not often been applied to them. We present a description and initial results of the Geophysical Astrophysical Spectral-element Adaptive Refinement (GASpAR) code, developed as part of the NCAR Geophysical Turbulence Program Initiative. Like most spectral-element codes, GASpAR combines the efficiency of finite-element methods with the accuracy of spectral methods, and it is designed to be flexible enough for a range of geophysics/astrophysics applications where turbulence or other complex multiscale problems arise.

There are several reasons why further progress in geophysical turbulence computation seems to require high-order adaptive methods. One group of reasons stems from the need for high spatial and temporal resolution. When the Reynolds number Re of a turbulent flow is large, nonlinear interactions dominate, and the effective number of degrees of freedom increases as $\mathsf{Re}^{9/4}$. Geophysical flows have Re as large as 10^8 to 10^{12}, and so the ability to simulate and examine the multi-scale behavior of geophysical flows depends critically on adequate resolution and/or parameterization of an even larger number of spatiotemporal scales. Theory demands that computations of turbulent flows capture a clear scale separation between the energy-containing inertial and the dissipative scale ranges. Convergence studies on compressible 3D flow computation show that to achieve the desired scale separation between the energy-containing modes and the dissipation regime using uniform-resolution grids, it is necessary to use at least 2048^3 cells [4]. Today such computations can barely be accomplished; a pseudospectral Navier-Stokes code on a grid of 4096^3 regularly spaced points has been run on the Earth Simulator [2] but their Re is still at most of the order of 10^6, still very far from what geophysics requires.

Another reason for high-order adaptivity is that it is not yet known what *flow structures* are key to understanding the remarkable statistical properties of turbulence (e.g., vortex

*Corresponding author: fournier@ucar.edu, 303-497-1614 (voice) 303-497-1646 (fax).

sheets, spirals or filaments, shocks or fronts, plumes, knots, helices or tubes). The link between structures and non-Gaussian statistics is the basis for the notion of intermittency, which plays a role in e.g., reactive flows, convective plumes, and solar coronal heating. Using traditional techniques, adequate resolution of structures requires extreme computational effort.

These considerations suggest that computational adaptivity is needed, provided the dynamically significant structures of the flow are sufficiently sparse that their dynamics can be followed accurately, although embedded in a noisy background.

We have built an object-oriented code, GASpAR, that is flexible enough to be applicable to a wide class of turbulent-flow and other multi-scale PDEs. The computational core is based on spectral-element operators, which are represented as objects. The PDEs are "weakly" formulated as volume integrals with piecewise polynomial test-function factors $\Phi_I(\vec{x})$ that are each continuous across the global domain, and that interpolate from global node values $\vec{X}_I$. The solution function is found in $\mathrm{span}_I\, \Phi_I$, by projecting there from the span of piecewise polynomial trial functions $\phi_j(\vec{x})$ that interpolate from local node values $\vec{x}_j$ but need not be globally continuous. The matrix $\Phi_I(\vec{x}_j)$ generalizes the Boolean "scatter matrix" used in the conforming-element formulation; thus this formulation accommodates both conforming and nonconforming elements, and the implementation includes data structures for handling inter-element communications across parallel processors. Nonconforming h-type dynamic adaptive mesh refinement is provided, and its suitability for turbulent flow models will be examined. The first application of the code will concern the Hwa-Kardar equations [1], which arise when writing the dynamical version of self-organized criticality. These equations can also serve as a model of solar flares when viewed as overlapping avalanches [3].

Acknowledgments: We are thankful to Huiyu Feng, Paul Fisher and Catherine Mavriplis for numerous helpful discussions, and to the CSS group at NCAR for early help in using spectral element methods.

References

[1] Hwa & Kardar 1992: *Phys. Rev. A* **45**, 7002.

[2] Isihara et al. 2003: *J. Phys. Soc. Japan* **72**, 983.

[3] Liu et al. 2002: *Phys. Rev. E* **66**, 056111.

[4] Sytine et al. 2000: *J. Comp. Phys.* **158**, 225.

A technique for diagnosing moisture dynamics in GCMs

Joseph Galewsky and Adam Sobel
Department of Applied Physics and Applied Mathematics,
Columbia University, New York, NY

Isaac Held
GFDL/NOAA
Princeton, NJ

A technique for diagnosing mechanisms controlling the water vapor distribution in a general circulation model (GCM) is presented. The technique involves defining a large number of tracers, each of which represents air which has last been saturated in a particular region of the atmosphere. The time-mean, zonal-mean tracer fields show the typical pathways that air parcels take between one occurrence of saturation and the next. Because saturation vapor pressure is a function only of temperature, and because mixing ratio is conserved for unsaturated parcels, these tracer fields can be used together with the temperature field to reconstruct the water vapor field. This method clarifies the separate influences of temperature and circulation on the water vapor field.

The technique is applied to an idealized GCM in which the dynamics are dry and forced using the Held-Suarez thermal relaxation, but the model carries a passive water-like tracer which is emitted at the surface and lost due to large-scale condensation with zero latent heat release and no condensate retained. The technique provides an accurate reconstruction of the simulated water vapor field. In this model, the dry air in the subtropical troposphere is produced primarily by isentropic transport, and is moistened somewhat by mixing with air from lower levels which has not been saturated since last contact with the surface. The authors suggest that the technique could be potentially useful in assessing the roles of temperature, circulation, and cloud microphysics in the maintenance of relative humidity in comprehensive GCMs

Anisotropic turbulence and zonal jets in the ocean, giant planets and computer simulations

Boris Galperin
College of Marine Science, University of South Florida, St. Petersburg, Florida

Semion Sukoriansky
Department of Mechanical Engineering/Perlstone Center for Aeronautical Engineering Studies, Ben-Gurion University of the Negev, Beer-Sheva, Israel

Hideyuki Nakano
Oceanographic Research Department, Meteorological Research Institute, Tsukuba, Ibaraki, Japan

Barotropic two-dimensional turbulence with Rossby waves is distinguished by strong anisotropy and energetic zonal jets in alternating directions. Flows on the β-plane and in thin shells on the surface of a rotating sphere develop strongly anisotropic spectrum with steep, n^{-5}, slope for the zonal flows and Kolmogorov-Kraichnan, $n^{-5/3}$, slope for the residuals. The n^{-5} zonal spectrum was found on all four giant planets of our solar system, both with regard to its slope and the amplitude. This spectrum can be used to analyze some basic characteristics of large-scale circulations on giant planets and for interplanetary comparisons. Recently, it was found that the mid-depth ocean currents in the North Pacific ocean also develop a system of alternating zonal jets and build up the same n^{-5} and $n^{-5/3}$ zonal and residual spectral distributions. The main characteristic of the planetary and oceanic flows under consideration is the smallness of their Burger number, $Bu = (L_d/R)^2$, where L_d is the first baroclinic Rossby radius of deformation and R is the planetary radius. Exploring the planetary-ocean analogy, we conclude that the fine-scale oceanic zonal jets are driven by strongly nonlinear, anisotropic dynamics of quasi-2D turbulence with Rossby waves and argue that the latitudinal scaling of these jets is determined by the large-scale friction processes.

I. ANISOTROPIC TURBULENCE ON GIANT PLANETS

Our previous simulations of barotropic two-dimensional (2D) turbulence on β-plane [1] and on the surface of a rotating sphere [2] have indicated that such flows give rise to strongly anisotropic spectra. In spherical geometry, with R being the radius of the sphere, Ω being its angular velocity, and n and m being the total and the meridional wave numbers, respectively, the following zonal ($E_Z(n)$) and residual ($E_R(n)$ spectral distributions are established:

$$E_Z(n) = C_Z(\Omega/R)^2 n^{-5}, \qquad m = 0, \quad n/n_\beta < 1, \quad (1)$$

$$E_R(n) = C_K \epsilon^{2/3} n^{-5/3}, \qquad \forall m \neq 0, \quad (2)$$

where $C_K \approx 6$ is the Kolmogorov-Kraichnan constant, $C_Z \simeq 0.5$, ϵ is the rate of the small-scale energy input, and $n_\beta = [(\Omega/R)^3/\epsilon]^{1/5}$ is the transitional wave number associated with the crossover between the spectra (1) and (2). The same spectral distributions were observed in steady-state simulations with a linear large-scale drag [3]. The latter paper also provides a detailed analysis of various interrelationships between the zonal and residual spectra.

The development of the flow regime with the spectra (1) and (2) is stipulated by fulfilling the requirement $n_{fr}/n_\beta \ll 1$, where n_{fr} is the wave number associated with the large-scale friction. This requirement is difficult to satisfy in the laboratory conditions and in the Earth atmosphere where friction with the underlying surface is high. However, the atmospheres of the giant planets may provide natural laboratories that can sustain such flows. Since the gas giants don't have solid boundaries, their friction and, therefore, n_{fr} are low. The requirement of the quasi-two-dimensionality is naturally fulfilled for the giant planets' atmospheres as the vertical thickness of the weather layers is much smaller than their horizontal extent. Another crucial requirement pertains to the value of the Burger number, $Bu = (L_d/R)^2$, where L_d is the first baroclinic Rossby deformation radius. It is well known that flows with $Bu \ll 1$ exhibit tendency to barotropization [4] and are, thus, likely to develop the spectral regime (1) and (2) if the criterion $n_{fr}/n_\beta \ll 1$ is also fulfilled. The existing data indicate that indeed, $Bu \ll 1$ for all four solar giant planets [5].

Using zonal velocity profiles obtained from the space stations Voyager 1 and 2 as well as from the Hubble Space Telescope, we have calculated the zonal spectra for all four solar giant planets in spherical representation; they are shown in Fig. 1. One can see a good agreement between the theoretical, Eq. (1), and observed zonal spectra for all four giant planets both with respect to the spectral slope and the amplitude (note that the data for Uranus is insufficient to establish the spectral slope but can be used to test the agreement in the amplitude).

One can observe that the slope -5 extends to some wave number which can be associated with n_{fr} and remains approximately level for $n < n_{fr}$. This zonal spectrum distribution allows one to analyze some large-scale characteristics of the atmospheric circulation on giant planets. By integrating Eq. (1) from 0 to ∞, obtain the total

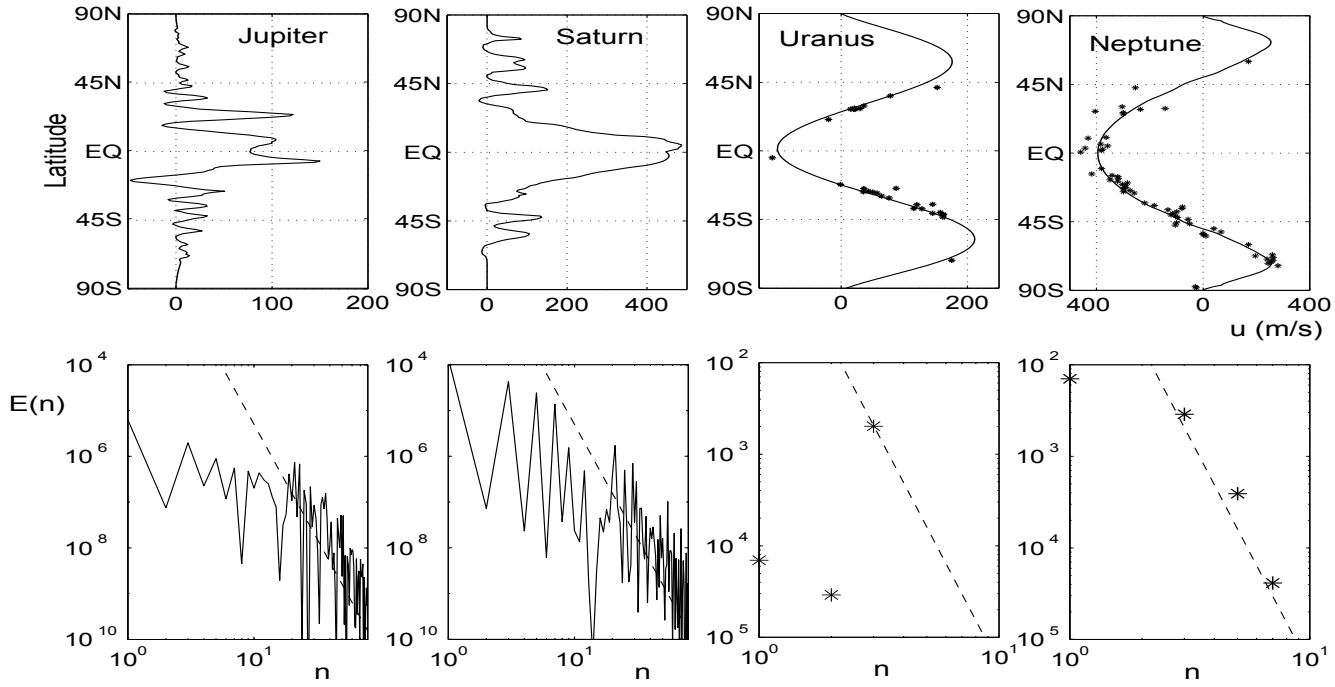

FIG. 1: Top row: observed zonal profiles deduced from the motion of the cloud layers [6–9]; bottom row: observed zonal spectra (solid lines and asterisks) and theoretical zonal spectra Eq. (1) (dashed lines) on the giant planets [all spectra are normalized with their respective values of $(\Omega/R)^2$].

kinetic energy of the circulation,

$$E_{\rm tot} = (5C_Z/4)(\Omega/R)^2 n_{fr}^{-4}. \qquad (3)$$

Equation (3) indicates that $E_{\rm tot}$ depends on R, Ω and n_{fr} only and does not depend on the rate of the energy injection ϵ. Being the only flow-dependent parameter in (3), the frictional wave number n_{fr} plays a paramount role in the global energetics.

II. ANISOTROPIC TURBULENCE IN THE OCEAN

In recent simulations with high resolution, eddy-permitting ocean general circulation model it was found that the mid-depth ocean currents in the north Pacific ocean also develop a system of alternating zonal jets and obey the zonal and residual spectral distributions (1) and (2). Since the Burger number in the ocean is small, one can infer that the planetary and sub-surface terrestrial ocean jets are generated and maintained by the same mechanism pertaining to quasi-2D turbulence with anisotropic inverse energy cascade. The connection between the planetary and terrestrial circulations sheds some new light on the basic properties of stability and variability of the large-scale flows in both systems.

[1] Chekhlov A., Orszag, S.A., Sukoriansky, S., Galperin, B. and Staroselsky, I.: The effect of small-scale forcing on large-scale structures in two-dimensional flows. *Physica D* **98**: 321–334, 1996.

[2] Huang, H.-P., Galperin, B. and Sukoriansky, S.: Anisotropic spectra in two-dimensional turbulence on the surface of a rotating sphere. *Phys. Fluids* **13**: 225–240, 2001.

[3] Sukoriansky, S., Galperin, B. and Dikovskaya, N.: Universal spectrum of two-dimensional turbulence on a rotating sphere and some basic features of atmospheric circulation on giant planets. *Phys. Rev. Lett.* **89**: 124,501–4, 2002.

[4] Salmon, S.: Lectures on Geophysical Fluid Dynamics. Oxford University Press, NY Oxford 1998.

[5] Menou, K., Cho, J. Y-K., Seager, S. and Hansen, B.M.S.: "Weather" variability of close-in extrasolar giant planets.

Astrophys. J. **587**: L113–L116, 2003.

[6] Garcýa-Melendo, E. and Sanchez-Lavega, A.: A study of the stability of Jovian zonal winds from HST images: 1995–2000. *Icarus* **152**: 316–330, 2001.

[7] Sanchez-Lavega, A., Rojas, J.F. and Sada, P.V.: Saturn's zonal winds at cloud level. *Icarus* **147**: 405–420, 2000.

[8] Hammel, H.B., Rages, K., Lockwood, G.W., Karkoschka, E. and de Pater, I.: New measurements of the winds of Uranus. *Icarus* **153**: 229–235, 2001.

[9] Sromovsky, L.A., Fry, P.M., Dowling, T.E., Baines, K.H. and Limaye, S.S.: Coordinated 1996 HST and IRTF imaging of Neptune and Triton III. Neptune's atmospheric circulation and cloud structure. *Icarus* **149**: 459-488, 2001.

Spectral modeling of internal waves and turbulence and its application in simulations of turbulent flows with stable stratification

Boris Galperin
College of Marine Science, University of South Florida, St. Petersburg, Florida

Semion Sukoriansky
Department of Mechanical Engineering/Perlstone Center for Aeronautical Engineering Studies, Ben-Gurion University of the Negev, Beer-Sheva, Israel

Veniamin Perov
Swedish Meteorological and Hydrological Institute, Norrköping, Sweden

A new model for turbulent flows with stable stratification is presented. This model belongs in the class of the quasi-Gaussian closures; its parameters are calculated based upon a self-consistent recursive procedure of small-scale modes elimination starting at the Kolmogorov scale k_d. The model includes both vertical and horizontal eddy viscosities and diffusivities thus explicitly recognizing the anisotropy induced by stable stratification. There are significant differences in the behavior of these turbulent exchange coefficients with increasing stratification. Generally, the vertical coefficients are suppressed while their horizontal counterparts are enhanced. The model accounts for the combined effect of turbulence and internal waves on the exchange coefficients. A dispersion relation for internal waves in the presence of turbulence is derived. A threshold criterion for the wave generation in the presence of turbulent scrambling is obtained. The new model can be used to derive subgrid-scale parameterizations for LES and eddy viscosities and diffusivities for RANS models. The latter approach is used to develop a new $K-\epsilon$ model which is tested in simulations of the atmospheric stable boundary layer (SBL) over sea ice. The new model performs well in both moderately and strongly stratified SBLs.

I. THE SPECTRAL MODEL

The spectral closure theory is developed for a fully three-dimensional, incompressible, turbulent flow field with imposed homogeneous, vertical, stable temperature gradient; the flow is governed by the momentum, temperature and continuity equations in Boussinesq approximation,

$$\frac{\partial \mathbf{u}}{\partial t} + (\mathbf{u}\nabla)\mathbf{u} + \alpha g\theta \hat{e}_3 = \nu_0 \nabla^2 \mathbf{u} - \frac{1}{\rho}\nabla P + \mathbf{f^0}, \quad (1)$$

$$\frac{\partial \theta}{\partial t} + (\mathbf{u}\nabla)\theta + \frac{d\Theta}{dz}u_3 = \kappa_0 \nabla^2 \theta, \quad (2)$$

$$\nabla \mathbf{u} = 0, \quad (3)$$

where $\mathbf{u}$ and θ are the fluctuating velocity and the fluctuating potential temperature, respectively; P is the pressure, ρ is the constant reference density, ν_0 and κ_0 are the molecular viscosity and diffusivity, respectively, α is the thermal expansion coefficient, g is the acceleration due to gravity directed downwards, $\frac{d\Theta}{dz}$ is the mean potential temperature gradient, and $\mathbf{f}^0$ represents a large-scale external energy source customarily used in spectral theories of turbulence; it maintains turbulence in statistically steady state and may originate from large-scale shear instabilities. According to Kolmogorov theory of turbulence, the details of this forcing are immaterial in statistical description; its net effect is communicated to the fluid via a single integral parameter, the rate of the energy injection at large scales. Due to strong nonlinear interactions, the external forcing excites all Fourier modes down to the dissipative scale k_d. The modes exert indiscriminant, random agitation upon each other which manifests as a stochastic *modal* forcing $\mathbf{f}$. This forcing is used to replace the non-linear equations (1), (2) by modal stochastic equations

$$u_i(\mathbf{k},\omega) = G_{ij}(\mathbf{k},\omega) f_j(\mathbf{k},\omega), \quad (4)$$

$$\theta(\mathbf{k},\omega) = -\frac{d\Theta}{dz} u_3(\mathbf{k},\omega) G_\theta(\mathbf{k},\omega), \quad (5)$$

also known as the Langevin equations. Here, $G_{ij}(\mathbf{k},\omega)$ and $G_\theta(\mathbf{k},\omega)$ are the velocity and the temperature Green functions, respectively. They include terms accounting for the damping of a given mode by all other modes due to nonlinear interactions. Eventually, these terms are associated with k-dependent viscosities and diffusivities [1, 2]. The Langevin equations can be viewed as a device that facilitates the replacement of the original nonlinear Navier-Stokes and temperature equations by a system of linear, forced, stochastic equations in which the energy budget is systematically adjusted for every Fourier mode. In more rigorous interpretation, the replacement of the fully nonlinear Navier-Stokes equations by the Langevin equations represents a *mapping* of the original flow field onto a quasi-Gaussian field $\mathbf{f}(\mathbf{k},\omega)$ under the constraints of incompressibility and conservation of the modal energy flux. In the case of neutral stratification, this approach recovers some basic features of isotropic homogeneous turbulence including the Kolmogorov spectrum [1].

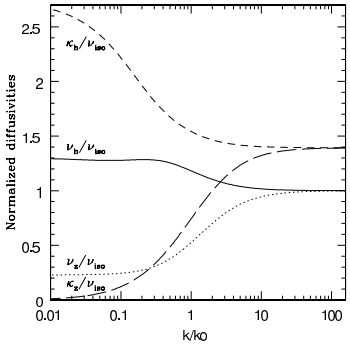

FIG. 1: Normalized horizontal and vertical eddy viscosities and diffusivities as functions of k/k_O.

The parameters of the eddy damping are calculated using a systematic algorithm of successive averaging over small shells of velocity and temperature modes. The algorithm consists of computation of small increments to the vertical and the horizontal viscosities and diffusivities generated by the averaging over small shells of the velocity and the temperature modes using the Langevin equations (4) and (5). It results in a system of four coupled ODEs for turbulent viscosities and diffusivities,

$$\frac{d}{dk}(\nu_h, \nu_z, \kappa_h, \kappa_z) = -\frac{\epsilon}{k^5} R_{1,2,3,4}(\nu_h, \nu_z, \kappa_h, \kappa_z), \quad (6)$$

where ϵ is the rate of the viscous dissipation; ν_h and ν_z are the horizontal and the vertical eddy viscosities, respectively; κ_h and κ_z are the horizontal and the vertical eddy diffusivities, respectively, and R_1 through R_4 are algebraic expressions. The procedure takes account of the combined effect of turbulence and internal waves. The computation starts at the Kolmogorov scale k_d where the initial values of the vertical and the horizontal viscosities and diffusivities are equal to their respective molecular values ν_o and κ_0 and is continued to an arbitrary wave number $k < k_d$. The system (6) can only be solved numerically. Solutions obtained for the non-dimensional variables $\nu_h/\nu_{\rm iso}$, $\nu_z/\nu_{\rm iso}$, $\kappa_h/\nu_{\rm iso}$ and $\kappa_z/\nu_{\rm iso}$ are presented in Fig. 1 as functions of the ratio k/k_O, where $k_O = (N^3/\epsilon)^{1/2}$ is the Ozmidov wave number and $\nu_{\rm iso}$ is the eddy viscosity for neutral stratification ($N = 0$) obtained with the same ϵ.

II. IMPLEMENTATION OF THE SPECTRAL RESULTS IN $K-\epsilon$ MODELING

The process of small scales elimination can be extended to the largest scales of the system, i.e., the integral length scale, k_L^{-1}. This approach is analogous to the Reynolds averaging and the resulting equations represent a sort of a RANS model. We have used ν_z and κ_z to develop a $K-\epsilon$ model based upon the spectral theory rather than the Reynolds stress closure. In simulations of SBLs, it was found necessary to generalize the formulation of the ϵ-equation given in [3] to include the effect of stratification in addition to the rotation,

$$C_1 = C_1^0 + C_f Ro_*^{-1} - C_N Fr_*^{-1}, \quad (7)$$

where $Ro_* = u_*/|f|L$, $Fr_* = u_*/NL$, u_* is the friction velocity, f is the Coriolis parameter, C_1^0 is the standard coefficient equal to 1.44, $L = 0.16K^{3/2}/\epsilon$ is the turbulence macroscale used in the $K-\epsilon$ modeling, $C_f = 111$ and $C_N = 0.58$ are empirical constants. The new $K-\epsilon$ model has been tested in simulations of ABL over sea ice and compared with the data from Beaufort Arctic Storms Experiment (BASE) and LES [4]. The results of the simulations with the new $K-\epsilon$ model are in good agreement with the LES for both cases of the moderate and strong stable stratification and provide significant improvement over the standard $K-\epsilon$ model.

[1] Sukoriansky, S., Galperin, B. and Staroselsky, I.: Cross-term and ϵ-expansion in RNG theory of turbulence. *Fluid Dyn. Res.* **33**: 319–331, 2003.

[2] Sukoriansky, S. and Galperin, B.: A spectral closure model for turbulent flows with stable stratification. In: *Marine Turbulence - Theories, Observations and Models*, H. Baumert, J. Simpson, J. Sundermann, eds., Cambridge University Press, in press.

[3] Detering, H. and Etling, D.: Application of the $E-\epsilon$ model to the atmospheric boundary layer. *Boundary-Layer Meteorol.* **33**: 113–133, 1985.

[4] Kosovic, B. and Curry, J.A.: A large eddy simulation study of a quasi-steady, stably stratified atmospheric boundary layer. *J. Atmos. Sci.* **57**: 1052–1068, 2000.

Simple Dynamical and Stochastic Models of Annular Patterns of Variability and the North Atlantic Oscillation

Edwin P. Gerber
with
Geoffrey K. Vallis

April 14, 2004

We present a hierarchy of simple models for the basic spatial and temporal structure of the large scale modes of intraseasonal variability in the extra-tropical atmosphere and associated variations of the zonal index. We focus on those patterns characterized by a meridional dipole structure of zonal wind and geopotential height, specifically the North Atlantic Oscillation (NAO) and a more zonally symmetric pattern known as the annular mode. Such patterns may be produced by momentum fluxes associated with large-scale mid-latitude stirring, such as that provided by baroclinic eddies. We probe the potential effects of this stirring with three models of varying complexity.

The spatial structure of the variability is illustrated with two stochastic models. The first is purely stochastic, an idealized, analytic model of the zonal wind. The second is dynamical, a barotropic model where midlatitude stirring is represented by a simple stochastic forcing. Both suggest that the NAO and annular modes are produced by the same mechanism, and thus are manifestations of the same phenomenon. While the time behavior of the low frequency patterns in the barotropic model captures the basic structure observed, the nature of the stochastic forcing precludes feedback from the low frequency modes on the high frequency stirring. A simplified three-dimensional primitive equation model allows for two way interaction between the the stirring - now baroclinic instability - and the variability, providing a richer context for understanding the temporal structure.

We develop and apply a new technique to estimate the distribution, total mass, and air-sea flux of anthropogenic carbon in the ocean. The technique exploits the fact that transport from the surface to the interior can be summarized in terms of Green functions that have a physical interpretation as distributions of transit times. We use measurements of inert tracers to constrain models of the transit-time distribution that accommodate a range of diffusive-mixing scenarios. The transit-time distributions are then used to propagate to the interior the surface-water history of anthropogenic carbon estimated in a way that includes temporal variation in CO_2 air-sea disequilibrium. By allowing for mixing in transport and for variable air-sea disequilibrium, we remove two sources of positive bias common in other studies. Our first application is the Indian Ccean, where we estimate that the anthropogenic carbon mass was 14.3–20.5 Gt in 2000, and the net air-sea flux was 0.26–0.36 Gt/yr. The upper bound of this range, the no-mixing limit, agrees well with previous studies, while the lower bound, the strong-mixing limit, is significantly below previous studies. Use of independent tracers in combination suggests that the lower, strong-mixing limit is more realistic.

VISCO-ELASTIC DAMAGE RHEOLOGY MODEL: THEORY AND EXPERIMENTAL TESTS

Yariv Hamiel (1), Yunfeng Liu (2), Vladimir Lyakhovsky (3), Yehuda Ben-Zion (2), Dave Lockner (4)

(1) Institute of Earth Science, The Hebrew University of Jerusalem, Israel. (2) Department of Earth Sciences, University of Southern California, Los Angeles, CA, USA. (3) The Geological Survey of Israel, Jerusalem, Israel. (4) U.S.G.S., MS 977, 345 Middlefield Rd., Menlo Park, CA, 94025, USA

We present a visco-elastic damage rheology model that provides a generalization of Maxwell visco-elasticity to a non-linear continuum mechanics framework incorporating material degradation and recovery, transition from stable to unstable fracturing, and gradual accumulation of non-reversible deformation. The model is a further development to the damage rheology framework of *Lyakhovsky et al.* [1997] for evolving effective elasticity. Our approach provides a quantitative treatment for macroscopic effects of evolving distributed cracking with local density represented by an intensive state variable. This assumes a system with a large number of cracks where one can define a smooth distribution over a representative volume that is much larger than the size of a typical crack and much smaller than the size of the entire domain. The present formulation, based on thermodynamic principles, leads to a system of kinetic equations for the evolution of damage. We introduce an effective viscosity inversely proportional to the rate of damage increase to account for gradual accumulation of irreversible deformation due to dissipative processes. A proposed power-law relation between the damage variable and elastic moduli leads to a non-linear coupling between rate of damage evolution and the damage variable itself. This allows the model to reproduce a transition from stable to unstable fracturing of brittle rocks and hysteresis phenomena including the Kaiser effect. Analytical solutions and 3-D numerical simulations based on the model formulation account for the main features of rock behavior under large strain. Model parameters are constrained using triaxial laboratory experiments with low porosity Westerly granite and high porosity Berea sandstone samples. During three of the laboratory experiments, small loading-unloading cycles were carried out. Throughout all of these cycles, acoustic emissions were not recorded and irreversible strain was not accumulated. These and other features of the laboratory data are compatible with the model predictions and provide experimental support for the model.

Baroclinic eddy life cycles and the potential role for mid latitude climate.

Various observational studies suggest that changes in synoptic scale eddy momentum fluxes are central to the dynamics of the leading modes of variability in midlatitudes: the North Atlantic Oscillation and the Annular Mode. In addition, there is evidence that momentum fluxes play an important role in the response of midlatitudes to external forcing. Examples include the effects of the stratosphere, ENSO, and midlatitude SST on midlatitude dynamics.

Observational and model studies have shown that there are various types of nonlinear wave life cycles, which differ in the way in which the eddies exchange momentum with the mean flow. Modeling studies also suggest that the transition from one type of life cycle to another entails a large change in eddy momentum flux, for a relatively small change in the basic flow.

It is therefore of great potential importance to understand what determine the type of life cycle an eddy will go through. We will present some results which suggest the wave life cycle is determined by the wave geometry of the mean flow during the linear growth stages, with the most important parameter being the phase speed of the waves. This raises the need to understand what controls the phase speed of baroclinically unstable waves.

Statistical inversion of oceanographic tracer data

Radu Herbei
Florida State University

Ian W. McKeague
Florida State University

Kevin Speer
Florida State University

McKeague, Nicholls and Speer (2003) introduced a statistical approach to the inversion of tracer data to estimate quasi-horizontal flow in an abyssal neutral density layer. A two-dimensional geostrophic flow model along with Markov chain Monte Carlo (MCMC) techniques are used to reconstruct the flow in a region of the South Atlantic. A PDE solver was used to compute numerical solutions of the advection-diffusion equations for the forward problem.

The present work extends this approach by adding vertical structure into the model. We develop a quasi-3D model to reconstruct vertical flow, as well as horizontal flow, and to provide improved maps for tracer concentrations. At least five layers (two above and two below the layer of interest) are needed to compute the vertical gradients of the neutral density which play a key role in the inversion.

We use bias-corrected hydrographic data, as compiled by Thurnherr and Speer (2004), with the tracer concentrations restricted to a thin constant neutral density layer (rather than a layer of constant depth). We focus on the $27.98 - 28.01$ neutral density layer which roughly corresponds to depths of 2000m $\pm$ 200m. In the pre-processing stage, the data are filtered to eliminate outliers, then interpolated to the nearest points in a regular lattice (see Figure 1).

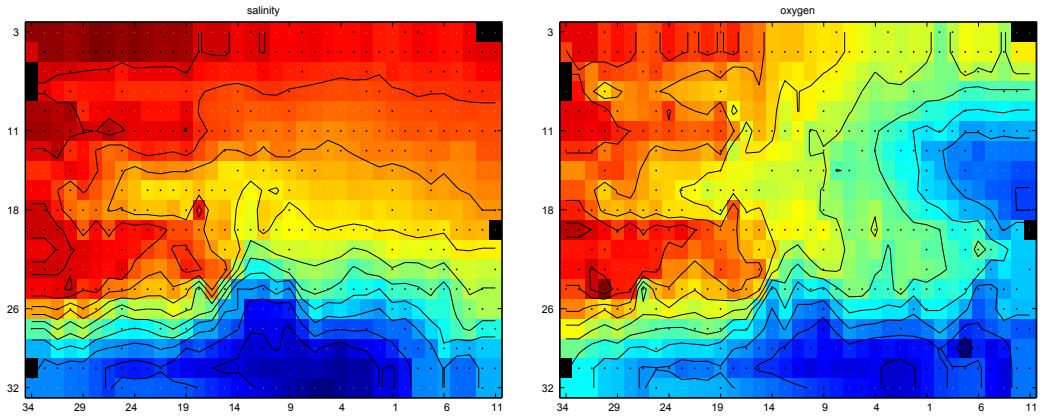

Figure 1: Interpolated salinity and oxygen concentrations. The dots indicate sites used in the inversion.

Let Ω be the domain of interest. The forcing in our model is the vertical diffusivity $\kappa^{(z)}$ (whereas McKeague, Nicholls and Speer (2003) used v) which creates the dynamics through an advection-diffusion equation $\underline{u} \cdot \nabla\gamma = \nabla \cdot (K\nabla\gamma)$ for the neutral density γ. Under the assumption that the zonal flow along the eastern boundary vanishes, using the linear vorticity equation $v = \frac{f}{\beta}\frac{\partial w}{\partial z}$, and geostrophic balance, we can express u as $u(x,y) = \int_x^{x_e}(\frac{\partial v}{\partial y} + \frac{\beta}{f}v)dx'$.

Given the parameters $\Phi = (\kappa^{(z)}, \kappa^{(x)}, \kappa^{(y)}, \lambda, C_{\partial\Omega})$, where λ is the oxygen consumption rate, the forward problem of solving the advection-diffusion equation for a tracer field C is handled using a 3D PDE solver (MUDPACK).

We use an observational model $C_i^{\text{obs}} = C_i^{\text{true}} + \varepsilon_i,\ i = 1, \ldots, n_D$ where i indexes a site on the lattice where data is available (the dots in Figure 1). The errors ε_i are assumed to be zero-mean independent Gaussian random variables with constant variance. A two-dimensional random field for $\kappa^{(z)}$, exponentially distributed horizontal diffusivities, and a Gaussian Markov random field for each tracer concentration C over the boundary $\partial\Omega$ are selected as priors. Bayes formula then gives the un-normalized posterior density of Φ conditionally on the tracer data, $\pi(\Phi|C) \propto L(C|\Phi)\pi(\Phi)$, where L denotes the likelihood. Reversible jump MCMC techniques are used to sample from this posterior distribution. Results are displayed in Figure 2.

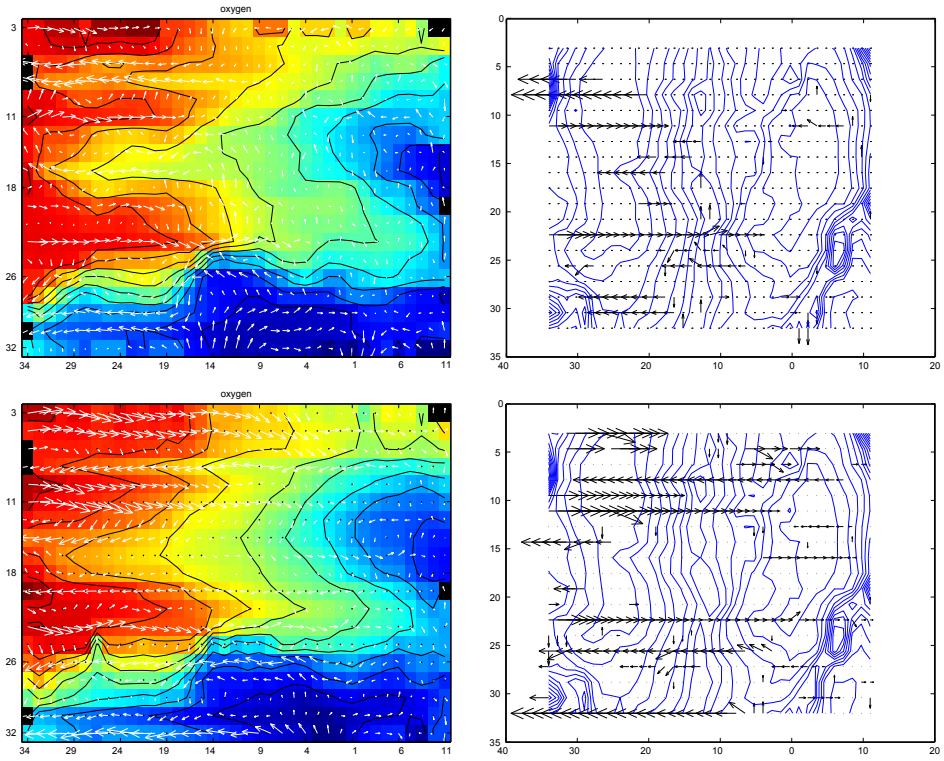

Figure 2: Reconstructed (posterior mean) oxygen concentration and advection (left) and significant flow (right) for the 28.00 neutral density layer, in the 2D case (upper, as in McKeague, Nicholls and Speer, 2003) and the quasi-3D case (lower).

References

McKeague, I. W., Nicholls, G. and Speer, K. (2003). Statistical inversion of South Atlantic circulation in an abyssal neutral density layer. *J. Mar. Research*, tentatively accepted, http://www.stat.fsu.edu/~mckeague/ps/jmr-submitted.pdf.

Thurnherr, A. M. and Speer, K. (2004). Representativeness of meridional hydrographic sections in the western South Atlantic. *J. Mar. Research.*, in press.

Saswata Hier-Majumder, Perry H. Leo, David L. Kohlstedt

May 17, 2004

Abstract

In this work, we analyze wetting of grain boundaries in a polycrystalline aggregate by fluid in triple grain junctions in response to an applied shear stress. We evaluate the local stress concentrations near fluid-filled triple grain junctions and along the grain boundaries. The fluid pressure at the solid-fluid interface is evaluated in terms of the local stress concentration and the solid-solid and solid-fluid interfacial energies. In this model, the applied stress results in a pressure gradient within the volume of the fluid, which drives the pore fluid down the pressure gradient. We also discuss the coupling between the rate of relaxation of normal stress by diffusion along the grain boundaries and the velocity of fluid penetration along grain boundaries, as well as the extent to which wetting of grain boundaries is controlled by both diffusive stress relaxation and wetting. In this formulation, we define the non-dimensional fluid mobility number β. For systems with low values of β, stress relaxes entirely by diffusive transport without wetting. For systems with high values of β, partial to complete wetting of grain boundaries is achieved, depending on the net interfacial energy at the tip of the fluid.

The results from our numerical experiments indicate that fluid is expelled from the boundaries under localized compressive normal stress and penetrates into the boundaries under localized tensile normal stress to relax the stress. As a result, a pore fluid network of tubules along grain edges transforms into a network of fluid planes along grain boundaries, altering the permeability of the aggregate. Such a coupling between the stress tensor and the permeability tensor in deforming polycrystalline solid-fluid aggregates needs to be further investigated in order to model fluid segregation and demixing in the planetary interiors.

On the importance of disequilibrium degassing for volcanic eruptions

J. Johnson, A. Proussevitch, and D. Sahagian (University of New Hampshire)

ABSTRACT

We investigate small-magnitude volcanic eruptive events to provide insight into the importance of diffusive degassing during volcanic eruptions. Our numerical code simulates transient fragmentation events, typical for the Strombolian and Vulcanian activity produced by volcanoes with silicic magmas. In our model simulations, we analyze explosions instigated by rapid depressurization of the entire conduit, such as might be caused by rapid unloading. For this type of trigger, we discover that eruption dynamics are heavily influenced by the continued exsolution of magmatic volatiles during eruption time scales (seconds to minutes). However, we demonstrate that for transient eruptive events, maintaining the dissolved gas content at a pressure-dependent solubility threshold is unrealistic. This important result contradicts many existing models, which assume equilibrium degassing during eruption. We demonstrate that for discrete, small-magnitude eruptions, equilibrium degassing provides too much 'fuel' and can not occur at the short time scales characteristic of most Strombolian and Vulcanian activity. Realistic numerical simulations for transient eruptive events must then incorporate more gradual gas exsolution, which depends primarily upon magma diffusivity, bubble density, ambient pressure, and volatile distribution. In our eruptive flow models, we introduce and incorporate analytical simplifications for diffusive bubble growth that is based upon previous, more complex, models. Finally, we show that complete disequilibrium degassing, in which no significant exsolution occurs on the time scale of the eruption, is a plausible scenario for discrete explosive events at many volcanoes with viscous magmas.

Computational Geodynamics with PETSc

Richard Katz, Matt Knepley & Marc Spiegelman

PETSc, the Portable Extensible Toolkit for Scientific computation, represents the leading software framework for the numerical solution of PDEs on parallel computers. We demonstrate the functionality, scalability and extensibility of PETSc using three simple examples relevant to computational geodynamics: (1) Creeping mantle flow and transport of heat in a subduction zone with a non-Newtonian, pressure and temperature dependent viscosity. (2) Stress driven melt segregation and shear localization in partially molten mantle rock. And (3) implementation of an efficient, parallel semi-Lagrangian advection scheme in PETSc.

Several factors are responsible for an expanding reliance on computational methods for the solution of PDE-based geodynamical models. First, these models are increasingly called upon to include complex, non-linear rheologies. Second, modern problems are marked by the need to resolve a wide range of length scales: from the entire mantle of the Earth, to the scale of a fault, to the scale of crystalline grains. While no current models span this entire range, dynamical processes of interest may occupy some fraction of it, requiring significant resolution and hence computational power and memory in excess of that available on a single processor. User-friendly software libraries containing robust linear and non-linear equation solvers that scale to the size of modern parallel computers are thus needed for the advancement of computational geodynamics.

The simulation shown here employ the PETSc framework from Argonne National Laboratory. Using the PETSc DA object, which is an abstraction for parallel, structured grid computations, we need only specify our discretized finite difference/volume equations. The Jacobian and Rhs vector are automatically allocated and assembled. The linear and nonlinear solvers are also abstracted to hide the parallel programming and allow for choice of solution method on the command line. These abstraction layers allow a portable, scalable parallel code to be built from the almost exclusively serial specification of the stencil. We will present scalability results for this code using the Argonne's linux cluster, Jazz.

Short-term earthquake prediction by reverse tracing of lithosphere dynamics

Abstract

V. Keilis-Borok and P. Shebalin

1. Most of existing earthquake prediction methods are aimed at intermediate-term and long-term predictions, with a lead time *years and tens of years* respectively. Here, we describe a new methodology for the short-term (*months* in advance) prediction. It is named Reverse Tracing of Precursors (*RTP*), since it traces premonitory phenomena in reverse order of their appearance.
2. Prediction is aimed at the "space-time of an alarm", that is the area and time interval, within which a target earthquake will occur. Unlike the classical problem of predicting continuous processes, our problem is predicting the rare point events; the predictor is a discrete sequence of alarms, while predictor of continuous processes is also a continuous function. Probability of errors is estimated on the basis of error diagrams.
3. RTR consists of two steps. First we detect the "candidates" for short-term precursors. Those are newly introduced chains of small earthquakes that reflect the premonitory increase of the earthquakes' correlation range; qualitatively, these chains are the dense, long, and rapidly formed sequences of small and medium earthquakes. We have found that such candidates precede within months most of the target earthquakes. However, up to 90% of the chains are not followed so closely by strong earthquakes and in prediction they would cause false alarms. Their rate is reduced on the second step. We determine whether certain intermediate-term precursors have occurred in the vicinity of each candidate within few years preceding it. If (and only if) yes, the chain is regarded as a precursor. Then a short-term alarm is declared in the vicinity of the chains for several (so far - nine) month.
4. San Simeon earthquake in Central California (magnitude 6.5, Dec. 22, 2003) and Tokachi-oki earthquake in Northern Japan (magnitude 8.1, Sept. 25, 2003) have been predicted by this methodology six and seven months in advance, respectively. Retrospective application of RTP to 25 more strong earthquakes in California, Japan, Eastern Mediterranean, and Italy is also encouraging. Decisive validation of methodology requires further advance predictions.
5. *Physical model* underlying *PRT* stems from the basic conditions of generation of an earthquake: accumulation of sufficient energy that the earthquake will release; and accumulation of sufficient instability triggering this release. Energy is carried by the *stress* field, instability – by the (*stress minus strength*) field. Here, we detect both processes by of premonitory seismicity patterns, found in the modeled and observed seismicity. Chains signal the fast surge of instability. Intermediate-term patterns show that this rise was preceded by accumulation of energy and instability in the same area over preceding years.
6. *Methodological advantage of RTP* over a direct analysis is in drastic reduction in dimensionality of parameter space where precursors are looked for. We have found here the precursors formed in narrow areas different from case to case, whose shape might be complicated, and size - diverse. Search for these areas by usual trial-and-error procedure would require trying one by one different shapes, sizes, chains and locations, which is hardly realistic. Reverse analysis resolves this impasse, determining from the start a limited number of the areas to consider.

7. *On other data*. It seems promising to apply *RTP* to other data relevant to earthquake prediction, such as InSAR, GPS, electromagnetic fields, fluid regime…. The first highly successful applications have been obtained with precursors gauging *interaction between the ductile and brittle layers of the Earth crust*; this established an important link of geodynamics and nonlinear dynamics.

8. *On other disasters*. The principles of *RTP* are not specific to earthquakes and might be applicable to critical transitions in a wide class of hierarchical non-linear systems.

9. Results, reviewed in this talk are described in the following papers:

- Aki, Keiiti, 2003. Introduction to Seismology for Earthquake Prediction. Preprint, Proc. of the Seventh Workshop on Non-Linear Dynamics and Earthquake Prediction, International Center for Theoretical Physics, Trieste.
- Gabrielov, A., Zaliapin I., Newman W., and Keilis-Borok, V., 2000. Colliding cascades model for earthquake prediction, Geophysical Journal International, 143, pp. 427-437. http://www.math.purdue.edu/~agabriel/cc2.pdf
- Keilis-Borok, V., Shebalin, P., Gabrielov, A., and Turcotte, D., 2004. Reverse detection of short-term earthquake precursors, Physics of the Earth and Planetary Interiors. In print. http://www.sciencedirect.com/science?_ob=GatewayURL&_method=citationSearch&_uoikey=B6V6S-4CG0SN6-1&_origin=SDEMFRASCII&_version=1&md5=b71d74d3de7f9566042390b93f4e643f
- Shebalin, P., Keilis-Borok, V., Zaliapin, I., Uyeda, S., Nagao, T., and Tsybin, N., 2004. Short-term advance prediction of the large Hokkaido earthquake, September 25, 2003, magnitude 8.1: A case history, Earth, Planets and Space. In print. Preprint: http://www.geocities.co.jp/Technopolis/4025/030925eq.pdf
- Zaliapin, I., Keilis-Borok, V.I., and Axen, G., 2002. Premonitory spreading of seismicity over the faults' network in southern California: Precursor Accord. J. Geophys. Res., 107(B10): 2221.
- Zaliapin, I., Keilis-Borok, V., and Ghil, M., 2003. A Boolean delay equation model of colliding cascades. Part II: Prediction of critical transitions, Journal of Statistical Physics, 111, pp. 839-861. http://www.igpp.ucla.edu/mcdonnell/papers/bde2s.ps

Earlier studies in the adjacent problem of intermediate-term prediction are reviewed in:

- Keilis-Borok, V., 2002. Earthquake prediction: state-of-the-art and emerging possibilities, Annu. Rev. Earth Planet. Sci., 30, 38 p. http://arjournals.annualreviews.org/doi/full/10.1146/annurev.earth.30.100301.083856
- Keilis-Borok, V. I., and Soloviev, A. A. (eds.), 2003. Nonlinear Dynamics of the Lithosphere and Earthquake Prediction, Springer-Verlag, Heidelberg, 337 p.

G.V. Kiryan, D.G. Kiryan,

Motion of the Earth's Center of Mass. Physical Principles.

St.Petersburg, 2003

keywords: Instantaneous Earth's center of mass, Motion of the Geocenter, Earth rotation parameters, polar motion, geocentric coordinates, secular drift, Chandler wobble, Kimura, metrology, astronomy, latitude, precession-nutation, zenith tube, liquid-metal mirrors, gravimetry, satellite navigation, geodynamics, Earth's core.

Abstract

The work describes main results obtained in studies of the trajectory of motion of the Earth's pole of rotation presented in the form of coordinate series IERS. These series generalize observational data collected by several generations of researchers.

The authors have found that the trajectory (polhode) of the Earth's rotation pole calculated via star coordinates corrected for nutation and precession reflects the motion of the Earth's center of mass.

The observed and measured motion of the Earth's center of mass in the space of objects is, in essence, a partial solution of the *N*-body problem of gravitational interaction.

The physics of variations in the coordinates of an observation place in astronomical studies has been revealed. The authors have shown that variations in the coordinates of the place are a joint manifestation of such physical phenomena as the motion of the Earth's center of mass within the Earth's body and tidal processes in the upper layers of the Earth's atmosphere. The book discusses the cause-effect relations between these phenomena and material Universe.

Formulae that can be used to calculate corrections for the motion of the Earth's center of mass in astronomical observations of coordinates of stars have been derived. Working correction equations were thoroughly tested. Comparative analysis of the calculated variations in the star latitudes and those observed during the period 1862–1984 has shown that the suggested physical model and also its mathematical equivalent adequately describe such a phenomenon as the motion of the Earth's center of mass within the Earth's body.

In the work, a number of basic applied scientific problems of monitoring the motion of the Earth's center of mass have been formulated.

Due to monitoring, a researcher can observe the result of the actual effect of disturbing and restoring forces upon the mass of the Earth's consistent core. A dynamic equilibrium of disturbing and restoring forces determines the spatial location of the Earth's consistent core in the liquid shell of the outer core or the geocentric coordinates of the Earth's center of mass.

The revealed physical phenomenon, i.e., the motion of the Earth's center of mass within the Earth's body, is of great importance, since it concerns both fundamental and applied sciences.

An Analytic Solution of Steady Stokes Flow on a Rotating Spherical Cap

Hideaki Kitauchi*, Harper Simmons† and Motoyoshi Ikeda‡

*Frontier Research System for Global Change, 3173-25 Showamachi, Kanazawa-ku, Yokohama 236-0001

†International Arctic Research Center-Frontier, 930 Koyukuk Drive, Fairbanks, Alaska 99775-7335

‡Graduate School of Environmental Science, Hokkaido University, N10, W5, Sapporo 060-0810

April 14, 2004

Abstract

An analytic solution of steady linear viscous flow on a spherical cap (Figure 1) rotating about its center is obtained. An inflow and an outflow on the boundary of spherical section drive the fluid motion. The solution of the stream function $\psi(\vartheta, \varphi)$ is expressed as the Fourier series in longitude $\varphi \in [0, 2\pi)$ and the first-kind associated Legendre functions of complex degrees in colatitude $\vartheta \in [0, \vartheta_b]$.

Figure 2 shows contours of the stream function ψ in a frame rotating with the spherical cap ($\vartheta_b = \pi/9$) viewed from the north pole. We assume uniform flow within an inlet and an outlet. The centers of the inlet and outlet are placed at $\varphi = 0, \pi$, respectively, making the straight angle, and their inscribed angles are the same $\pi/9$. No-slip boundary condition is imposed. The inflow turns westward immediately after entering the spherical cap and separates into cyclonic and anticyclonic flows along the boundary. These two branches merge and turn eastward before exiting the outlet. The streamline passing through the center of the inlet passes the north pole and the center of the outlet; this divides the inflow into the above two branches. The results in part support the approximation analysis and laboratory experiment done by Imawaki and Takano (1974).

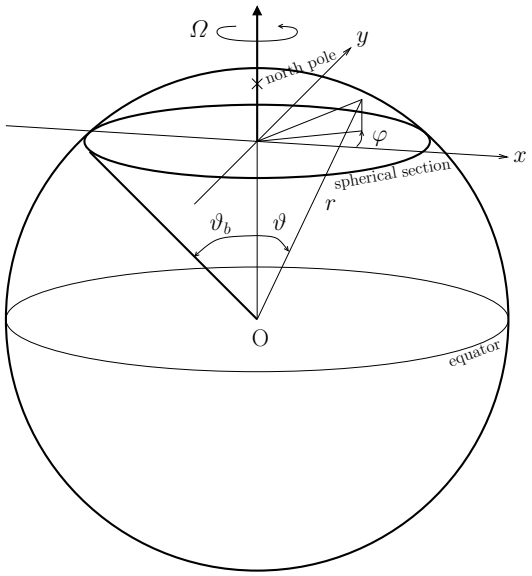

Figure 1: Configuration of a spherical cap.

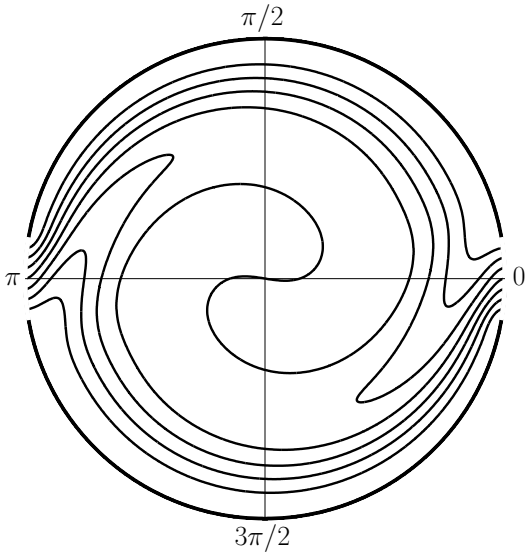

Figure 2: Contours of stream function $\psi(\vartheta, \varphi)$.

*E-mail: kitauchi@jamstec.go.jp

†E-mail: hsimmons@iarc.uaf.edu

‡E-mail: mikeda@ees.hokudai.ac.jp

Reduced atmospheric models: proper basis functions, dimensionality, replacing fast degrees of freedom by stochastic noise

Frank Kwasniok (f.kwasniok@lse.ac.uk)

Department of Statistics, London School of Economics, London, United Kingdom

The construction of reduced atmospheric models, i. e., models that explicitly deal only with a limited number of essential degrees of freedom while keeping as much realism as possible has attracted some attention in recent years. In the present paper, nonlinear reduced models of large-scale atmospheric dynamics are derived using a quasigeostrophic three-level spectral model, truncated to T30, with realistic variability as dynamical framework. The study focuses on three issues: (i) finding appropriate basis functions for efficiently spanning the dynamics and a comparison between different choices of basis functions; (ii) the minimal dimensionality of the reduced model necessary to faithfully reproduce certain aspects of the long-term behavior of the full spectral model; (iii) the question of whether the influence of unresolved fast-evolving degrees of freedom onto the resolved slowly-evolving large-scale degrees of freedom can be represented by stochastic terms.

In the first part of the study, nonlinear deterministic reduced models are obtained by projection of the equations of motion onto a truncated basis spanned by empirically determined modes. The total energy metric is used in the projection; the nonlinear terms of the low-order model then conserve total energy. Apart from retuning the coefficient of horizontal diffusion, no empirical terms are fitted in the dynamical equations of the low-order model in order to properly preserve the physics of the system. Using the methodology of principal interaction patterns (PIPs), basis functions are derived that are optimized to capture the strongly non-normal linear interactions between the mean state and the anomalies as well as the nonlinear terms. The optimized modes are calculated easily and robustly as eigenvectors of a linear eigenvalue problem. This eigenvalue problem is determined out of a class of eigenvalue problems using an only low-dimensional nonlinear search based on a dynamically motivated cost function. The mean state and the standard deviation of the sreamfunction as well as the momentum fluxes in the T30 model are well reproduced in a long-term integration by a PIP model with only about 50 modes; however, a correct modeling of probability distributions and especially spectral densities of the system requires a quite large number of modes. At any truncation level, reduced models based on PIPs are substantially superior to reduced models based on empirical orthogonal functions (EOFs) that have recently been proposed.

In the second part of the work, the reduced models are augmented by additive stochastic terms in order to represent the influence of neglected fast-evolving modes onto the resolved slowly-evolving modes. Both white and red noise processes are tested. The variances, correlation structure and autocorrelation functions of the noise terms are determined empirically from time series of the tendency errors of the deterministic low-order model. Again, the coefficient of horizontal diffusion is retuned for the stochastic model to exhibit in a long-term integration the same amount of variance in the resolved modes as the full spectral model. The noise terms lead to a great improvement of the performance of the reduced model over the deterministic reduced model.

Two-phase capillary flow through undulating tube

M. Latva-Kokko and D. Rothman

Department of Earth Atmospheric and Planetary Sciences, Massachusetts Institute of Technology, 77 Massachusetts Avenue, Cambridge MA 02139-4307

We study the drainage of a wetting fluid in a two-dimensional undulating capillary tube using the lattice Boltzmann method [1,2]. The method is modified in order to allow constant contact angle on the walls. The walls of the tube are given by sinusoidal functions. This tube acts as a simplified model of a two-dimensional fracture geometry and allows us to test the applicability of the lattice-Boltzmann method and gain insight into the dynamical aspects of capillary flow through natural fractures. The fluid starts at rest and the non-wetting fluid is injected into the tube from one end. We apply a constant pressure difference between the inlet and the outlet. This pressure difference is large enough to overcome the capillary forces even at the most narrow parts of the tube. The results are compared against quasistatic predictions given by the Washburn equation. For low driving forces the Washburn estimate of the velocity is followed and the interfacial pressure drop is given by the radius of curvature of the interface. We study the transition from quasistatic to dynamic flow. We plan to extend these studies to drainage in rough fractures.

[1] D. Rothman and S. Zaleski, *Lattice Gas Cellular Automata*, Cambridge University Press, Cambridge (1997).

[2] Y. Qian, D. d'Humières, P. Lallemand, Europhys. Lett. **17**, 479 (1992).

Orientational flow enhancement and inhibition in rough fractures

M. Latva-Kokko and D. Rothman

Department of Earth Atmospheric and Planetary Sciences, Massachusetts Institute of Technology, 77 Massachusetts Avenue, Cambridge MA 02139-4307

We have studied numerically the permeability of a rough fracture when viscous forces are dominating (low Reynolds number). The original fracture was studied experimentally and numerically by Y. Méheust and J. Schmittbuhl [1,2]. The experimental fracture consisted of a surface of fractured granite block and horizontal plexiglass plate. Theoretical and numerical studies have shown that a spatially varying aperture $d(x, y)$ forces fluid to follow tortuous paths through the fracture, and that this effect results in significant departures fromthe cubic law $K = \langle d \rangle^3/12$. Here $\langle d \rangle$ is the average aperture of the fracture and K is the transmittivity of the fracture.Hydrodynamic aperture can be defined as $d_h = (12K_{\text{measured}})^{\frac{1}{3}}$ whereas mechanical aperture is just $d_m = \langle d \rangle$. In the experiment the fracture was found to inhibit flow, i.e., $d_h < d_m$ in the x-direction, and to enhance flow, i.e., $d_h > d_m$ in the y-direction. We have confirmed these numerical and experimental results using a three dimensional Lattice-Boltzmann [3,4] simulations of Navier Stokes equations. These simulations take into account the potential z-directional fluid flows and have a capabibility of going to higher Reynolds numbers.

[1] Y. Méheust and J. Schmittbuhl, Geophys. Res. Lett. **27**, 2989 (2000).

[2] Y. Méheust and J. Schmittbuhl, J. Geophys. Res. **106**, 2089 (2001).

[3] D. Rothman and S. Zaleski, *Lattice Gas Cellular Automata*, Cambridge University Press, Cambridge (1997).

[4] Y. Qian, D. d'Humières, P. Lallemand, Europhys. Lett. **17**, 479 (1992).

An Inverse Spectral Element Ocean Model

J. Levin, D. Haidvogel, M. Iskandarani

A new ocean circulation model based on unstructured spectral finite element methods has been developed over the past few years. Its main advantages are: the flexibility inherent in its unstructured gridding, allowing it to easily handle complicated oceanic geometries; good scalability characteristics on parallel computers including Beowulf-class systems; and dual h-p paths to convergence.

We describe the planned development of a new inverse spectral element ocean model (I-SEOM), based upon the Inverse Ocean Model system developed by Bennett and Chua (OSU). The system is targeted at the study of idealized coastal ocean processes (downslope flows, bottom boundary turbulence, cross-shelf pumping, the role of canyons, etc.), using reference datasets obtained from laboratory experiments (e.g., at the Coriolis Laboratory in Grenoble, France) and from in situ coastal ocean observing networks (e.g., the U.S. Northeast Observing System). As a first step in the development of I-SEOM, we describe the tangent-linear and adjoint systems for the two-dimensional (shallow water) dynamical engine of SEOM. We review the 4D-variational assimilation algorithm being employed, and show some initial test results.

Threshold phenomena in erosion driven by subsurface flow

Alexander Lobkovsky[1], Bill Jensen[2], Arshad Kudrolli[2], Daniel H. Rothman[1]

[1]*Department of Earth, Atmospheric, and Planetary Sciences Massachusetts Institute of Technology, Cambridge, MA 02119*

[2]*Department of Physics, Clark University, Worcester, MA 01610*

Erosion is mobilization of granular material by a fluid flowing over or through it. The former case, erosion driven by overland flow, is relatively well studied compared to erosion driven by subsurface seepage flows. We study a laboratory-scale experiment in which all aspects of seepage erosion are present. We observe steady-state flow of water through a pile of glass beads, emergence of surface water and sediment flow, channelization instability, and growth and coarsening of the resulting channel network. We use this experiment to test theories of sediment dynamics. For example, the onset of flow is controlled by competition of the hydrodynamic forces on a grain and the stabilizing effect of the grain's weight. Seepage flow creates an additional source of hydrodynamic stress which radically alters the phenomenology of the onset of sediment motion. In overland flow, a finite flux is required to erode a slope less steep than the angle of repose. On the contrary, we show that there exists a critical slope significantly smaller than the angle of repose for which *any* seepage flux will mobilize sediment.

A visco-elastic damage rheology and rate- and state-dependent friction

Vladimir Lyakhovsky[1], Yehuda Ben-Zion[2] and Amotz Agnon[3]

[1] Geological Survey of Israel, Jerusalem 95501, Israel; vladi@geos.gsi.gov.il
[2] Department of Earth Sciences, Univ. of Southern CA, Los Angeles, CA, 90089-0740, USA; e-mail: benzion@usc.edu
[3] Institute of Earth Sciences, Hebrew Univ. of Jerusalem, Jerusalem 91904 Israel; amotz@cc.huji.ac.il

We present relations between a visco-elastic damage rheology model and rate- and state-dependent (RS) friction. Both frameworks describe brittle deformation, although the former implies a deforming zone while the latter may be associated with sliding surfaces. At present, the most detailed description of rock friction is provided by the RS friction. This framework accounts for the evolution of frictional strength as a function of slip, slip-velocity and state variables that characterize properties of the sliding surfaces. The RS friction provides a conceptual framework incorporating the main stages of an earthquake cycle. However, this formulation does not provide a mechanism for possible evolution of the geometry and elastic properties of the deforming rocks. Such processes are accounted for in damage rheology models that generalize Hookean elasticity to inelastic brittle deformation by relating an intensive damage state variable to evolving elastic properties. Analyses of stress-strain and acoustic emission laboratory data during deformation leading to brittle failure indicate [*Hamiel et al.*, 2004] that the fit between model predictions and observations improves if we also incorporate gradual accumulation of a non-reversible deformation with a rate proportional to the rate of damage increase. Shear strain larger than a threshold value induces material degradation, while post-failure behavior under lower strain produces healing. This allows for an overall cyclic stick-slip motion along a narrow zone with localized damage. Each deformation cycle (limit cycle) can be divided into healing and weakening periods associated with decreasing and increasing damage, respectively. Analytical and numerical results demonstrate the connection between kinetic parameters of the damage rheology model and the frictional parameters (conventionally referred to as a and b). The direct effect and the magnitude of the frictional parameter a are related to the material strengthening with increasing rate of loading. The strength and residence time of asperities (elements) in a weakening stage depends on the rates of damage and irreversible strain accumulation. The transient stage and overall change in friction parameters (a-b) are controlled by the duration of the healing stage and asperity (element) strengthening during this stage. For a model with spatially variable properties, the damage rheology reproduces the logarithmic dependency of steady-state friction on both the sliding velocity and the normal stress. The transition from a velocity strengthening regime to a velocity weakening can be obtained by varying the rate of inelastic strain accumulation and keeping the other damage rheology parameters fixed.

Rheology of magmas and transition in lava flow dynamics inferred from percolation theory

Martin Saar
Department of Geological Science, University of Michigan (msaar@umich.edu

Michael Manga
Department of Earth and Planetary Science, University of California, Berkeley (manga@seismo.berkeley.edu)

Transport properties of multiphase materials may either reflect the deformation of a material as a whole under applied stress (rheology) or the transfer of some medium, such as fluids, within the material (conductivity). Both types of transport are fundamentally different and depend on the relevant material properties in different ways. However, rheology and conductivity of composite materials are both determined in part by the interconnectivity of their individual elements (objects) that constitute their phases.

Percolation theory describes interconnectivity of such objects in a random multiphase system as a function of the geometry, distribution, volume fraction, and orientation of the objects. The structure of the composite material may evolve with time due to chemical reactions or temperature changes. A critical threshold may be passed during the structural evolution and as a result some material properties such as yield strength or conductivity can change abruptly and may exhibit a power-law behavior above, and close to, the so-called percolation threshold.

Multiple processes in the Earth sciences may exhibit threshold properties and may thus be investigated employing percolation theory concepts. Examples include permeability changes in the crust or in the mantle due to partial melting, formation or closure of pores and fractures in solids, or growth and coalescence or degassing of bubbles in liquids. Similarly, the rheology of magmas can depend on the amount, geometry, and interconnectivity of the suspended crystals (Saar et al., EPSL, 2001) as described next in more detail.

We present continuum percolation results (Saar and Manga, Phys. Rev. E, 2002) for three-dimensional randomly oriented soft-core polyhedra (prisms) representing for example crystals in suspensions or fracture networks for rheology and permeability studies, respectively. The prisms are biaxial or triaxial and range in aspect ratio over 6 orders of magnitude. Percolation threshold results for prisms are compared with studies for ellipsoids, rods, ellipses, and polygons and differences are explained using the concept of the average excluded volume (Balberg et al., Phys. Rev. B, 1984). For large shape anisotropies we find close agreement between prisms and most of the above mentioned shapes for the critical total average excluded volume. Cubes exhibit the lowest shape anisotropy of prisms minimizing the importance of randomness in orientation with respect to percolation threshold results. We also derive an equation that allows scaling of percolation thresholds for suspensions of different particle shapes and with given respective average excluded particle volumes.

We provide an example from magma rheology (Saar et al., EPSL, 2001) as an application of the above continuum percolation results. The formation of a continuous crystal network in magmas and lavas can provide finite yield strength, τ_y, and can thus cause a change from

Newtonian to Bingham rheology. The rheology of crystal-melt suspensions affects geological processes, such as ascent of magma through volcanic conduits, flow of lava across the Earth's surface, melt extraction from crystal mushes under compression, convection in magmatic bodies, or shear wave propagation through partial melting zones. Here, three-dimensional numerical models are used to investigate the onset of 'static' yield strength in a zero-shear environment. Crystals are positioned randomly in space and can be approximated as convex polyhedra of any shape, size, and orientation. We determine the critical crystal volume fraction, ϕ_c, at which a crystal network first forms. The value of ϕ_c is a function of object shape and orientation distribution, and decreases with increasing randomness in object orientation and increasing shape anisotropy. For example, while parallel-aligned convex objects yield $\phi_c = 0.29$, randomly oriented cubes exhibit a maximum ϕ_c of 0.22. Approximations of plagioclase crystals as randomly oriented elongated and flattened prisms (tablets) with aspect ratios between 1:4:16 and 1:1:2 yield $0.08 < \phi_c < 0.20$, respectively. The dependence of ϕ_c on particle orientation implies that the flow regime and resulting particle ordering may affect the onset of yield strength and that ϕ_c in zero-shear environments is a lower bound for ϕ_c.

Dynamically balanced decade-mean global sea level at mesoscale resolution

Nikolai A. Maximenko [1] and Pearn P. Niiler [2]

[1] International Pacific Research Center, SOEST, University of Hawaii, USA
(nikolai@soest.hawaii.edu)
Also at P.P.Shirshov Institute of Oceanology, Russian Academy of Sciences, Moscow, Russia
[2] Scripps Institution of Oceanography, University of California, San Diego, USA
(pniiler@ucsd.edu)

Sea level together with Ekman currents largely defines surface circulation of the ocean. Horizontal velocities advecting and mixing properties of seawater work to compensate the effect of forcing by corresponding nonuniform in space and varying in time air-sea fluxes and thus they lend important stability to the entire Earth Climate system. Mean sea level associated with currents is essential for principal dynamical balances of the ocean, but is hard to observe. Its extreme values do not differ by more than 3 meters, while elevation of the equipotential surface (geoid) used as a reference varies due to mass distribution within the Earth from about -100 to +100 meters. Even most advanced models of the geoid (such as EGM96) based on decades of satellite and ground gravity measurements still contain error reaching in some areas many tens of centimeters, which was corrected only last year during the specially designed twin-satellites mission GRACE. Unfortunately, the GRACE model of the geoid does not resolve horizontal scales less than 500 km that imposes same limitation on resolution of the mean sea level referenced to that geoid. Such coarse resolution significantly distorts the pattern on most of oceanic fronts and jets, whose accurate representation is necessary for adequate description of mean ocean circulation.

In this study we managed to enhance the spatial resolution of the GRACE-based mean sea level using additional information from surface drifters, satellite altimeters and wind products. This information comes in form of estimates of the tilt of mean sea level using the momentum equation

$$\nabla\langle\eta\rangle = -\left(d\mathbf{V}/dt + \mathbf{f} \times (\mathbf{V} - \mathbf{V}_{ekman})\right)/g - \nabla\eta',$$

where velocity $\mathbf{V}$ and acceleration $d\mathbf{V}/dt$ are computed from trajectories of the Surface Velocity Program drifters with large drogues attached at 15m depth, and temporal anomaly of the sea surface tilt $\nabla\eta'$ is calculated using AVISO/Enact Merged Sea Level Anomaly maps.

Ekman currents $\mathbf{V}_{ekman}$ at 15 m are parameterized to the NCAR/NCEP reanalysis winds as the best fit of $\nabla\langle\eta\rangle$ smoothed to 9^0 in zonal and 3^0 in meridional direction to the GRACE-based mean sea level released by the NASA/JPL. Optimal formula of the parameterization reveals remarkable seasonal differences, with its parameters in summer corresponding well with the formula suggested by Ralph and Niiler (1999). In winter, both the angle between $\mathbf{V}_{ekman}$ and wind and the coefficient between their magnitudes decrease remarkably. Although qualitatively this tendency agrees with simple enhancement of mixing by a wintertime convection, such traditional models as KPP are not able to provide quantities that we observed in the data. We achieve satisfactory model of the mixing coefficient profile for winter season by modifying "the law of the wall" at the sea surface to simulate the effect of well-developed surf.

Thus obtained values of $\nabla\langle\eta\rangle$ combined within a single cost function with estimates of $\langle\eta\rangle$ in the NASA/JPL model provide precise description of mesoscale structures, some of which have been found amazingly complex even after averaging over ten years of observations. Maps of global mean sea level and mean surface velocities at fine mesoscale resolution show all known currents and also reveal some new features, which are to be validated by future studies.

A new kind of bedform

Brad Murray
Division of Earth and Ocean Sciences/Center for Nonlinear and Complex Systems
Duke University, Box 90320, Durham, NC, 27708, (919) 681-5069, abmurray@duke.edu
Rob Thieler
U. S. Geological Survey, Coastal and Marine Geology Program
384 Woods Hole Road, Woods Hole, MA, 02543-1598, (508) 457-2350, rthieler@usgs.gov

Numerous recent seabed observations have revealed that a striking type of large-scale pattern adorns many inner continental shelves around the world. The sediment in these environments is somehow segregated into swaths of coarse material (coarse sand and gravel), separated by domains of fine sand. Coarse swaths, usually on the order of 100 m wide, often extend kilometers in the offshore direction. Sharp boundaries separate coarse and fine domains. While the plan-view characteristics of this phenomenon vary considerably from one location to another, the pattern can be quite well ordered, reminiscent of well-organized bedforms such as wind ripples.

We present a hypothesis for the formation of these grain-size-sorted patterns, and an exploratory numerical model to test its plausibility. The hypothesis and model involve a feedback and subsequent emergent interactions that lead to an unusual kind of large-scale bedform. More familiar bedforms grow because the interaction between a topographic perturbation and a sediment-flux field cause the perturbation to grow. However, in our case, grain-size effects rather than topographic interactions drive the feedback and determine the behaviors of the resulting features.

The hypothesis begins with the observation that where a shallow seabed is covered by coarse material, that sediment is sculpted into large wave-generated ripples, with wavelengths commonly on the order of a meter. Wave motions interacting with these large roughness elements will generate large-scale, energetic turbulence. This enhanced turbulence will tend to enhance the entrainment of fine sediment, and to inhibit its redeposition locally. Then, any mean current will tend to advect the fine sediment to a location where the bed is finer, the wave-generated ripples are smaller, and the turbulence is less energetic. Starting from a nearly homogeneous seabed, these interactions will tend to preferentially remove fine sediment where the bed is coarser, and to preferentially deposit it where the bed is finer. This feedback will tend to produce a grain-size sorted pattern.

.

To investigate whether this feedback and subsequent interactions between sorted features could produce large-scale sorted patterns with the characteristics observed in nature, we have developed a simple numerical model. In this model, rather than explicitly simulating the hydrodynamics and sediment transport on the scales associated with wave-generated ripples, we parameterize the effects these processes have on larger-scale sediment transport; we treat transport as a function of bed composition, as a proxy for ripple size. The model robustly generates sorted patterns. The size and appearance can match those of the natural features, although the details of the patterns depend on the wave and current characteristics. As perturbations grow to finite amplitude, interactions between them, including mergers, lead to a larger-scale, better-organized pattern. The plan-view evolution of these ‘sorted bedforms’ appears surprisingly similar to the evolution of some topographically driven bedforms.

Petrological layering at 660km induced by multi-component phase changes in cooling Earth

Takashi Nakagawa

Department of Geophysical Sciences, University of Chicago

Numerical simulations of a coupled model of fully-dynamical thermo-chemical mantle convection and global heat balance in the core with the inner core growth and compositional convection have been conducted for understanding influences of the style of compositional stratification in the transition zone to the heat transfer by mantle convection. Two styles of compositional stratification have been found by using numerical model of thermo-chemical mantle convection: (1) filtering effects for upwelling plumes including dense material in pure olivine system [Weinstein, 1992] and (2) compositional stratification generated by the partial segregation of oceanic crust around the 660km [Tackley and Xie, 2003; Ogawa, 2003] which has been predicted by mineral physics experiments of realistic mantle material (combined between olivine system and pyroxene-garnet system; hereafter describing as 'combined system') [Irifune and Ringwood, 1993; Ono et al., 2001]. However, there have been no studies to investigate the difference for thermo-chemical evolution of a convecting mantle and core between pure olivine system and combined system which is dependent on the compositional field because former studies shown here have not been based on a coupled model of fully-dynamical thermo-chemical evolution in a convecting mantle and global heat balance in the core.

For a coupled model of fully-dynamical thermo-chemical mantle convection and global heat balance in the Earth's core, it is similar to our former paper [Nakagawa and Tackley, 2004]. In that study, the phase changes system has been assumed only pure olivine system, on the other hand, in this study, combined system is assumed. For composition-dependent phase change system, it is the same procedure as Tackley and Xie [2003] and Xie and Tackley[2004], which the density variation for buoyancy force is given as

$$\rho\left(f_{ol},z,T\right)=\left[f_{ol}\rho_{ol}\left(z,T_{ad}\right)+\left(1-f_{ol}\right)\rho_{px-gt}\left(z,T_{ad}\right)\right]\left[1-\alpha_{eff}\left(T-T_{ad}\left(z\right)\right)\Delta\rho_{th}\right] \quad (1)$$

where all notations for this equation can be found in Xie and Tackley[2004]. Initial conditions for temperature and chemical composition are assumed to be adiabatic temperature profile and uniform compositional field. Important parameter is the density difference between basaltic material and residual harzburgite material, which is approximately 2.1% at the CMB.

Time evolution for CMB temperature, heat fluxes through both boundaries and inner core radius indicates that combined system is better than pure olivine system as a result of thermal evolution of Earth's

core, which means that inner core radius is inside of 5km from our criteria (1220km), on the other hand, it is more than 600km from criteria for pure olivine phase system. However, for heat fluxes, strongly episodic features are found in combined system. Heat flux through the CMB in combined system is episodically below the minimum heat flux for maintaining the geodynamo process. Pure olivine system seems to be good for heat flux through the both boundaries. In order to check geochemical evolution for different phase systems in the uppermost lower mantle, there are various diagnostics but those results and interpretations will be appeared in the conference.

References

Irifune T., Ringwood, A.E., 1993, Phase-Transformations In Subducted Oceanic-Crust and Buoyancy Relationships At Depths Of 600-800 Km In the Mantle, Earth Planet. Sci. Lett., 117, 101-110.

Nakagawa, T., Tackley, P. J., 2004, Effects of thermo-chemical mantle convection on the thermal evolution of the Earth's core, Earth Planet. Sci. Lett., 220, 107-119.

Ogawa, M., 2003, Chemical stratification in a two-dimensional convecting mantle with magmatism and moving plates, J. Geophys. Res., 108, doi:10.1029/2002JB002205.

Ono, S., Ito, E., Katsura, T., 2001, Mineralogy of subducted basaltic crust (MORB) from 25 to 37 GPa, and chemical heterogeneity of the lower mantle, Earth Planet. Sci. Lett., 190, 57-63.

Tackley, P. J., Xie, S., 2003, Stag3D: A code for modeling thermo-chemical multiphase convection in Earth's mantle, Proceedings of the Second MIT Conference on Conputational Fluid and Solid Mechanics.

Weinstein, S. A., 1992, Induced compositional layering in a convecting fluid layer by an endothermic phase transition, Earth Planet. Sci. Lett., 113, 23-39.

Xie, S., Tackley, P. J., 2004, Evolution of Helium and Argon isotopes in a convecting mantle, Phys. Earth Planet. Int., in press.

Though modern four-dimensional data assimilation schemes, such as the Kalman Filter, are both powerful and bec oming increasingly necessary, it is well known that they are all based, to some extent, on assumptions of linear dyn amics. Much research has thus focused on the feasibility of these assumptions, and ways to rectify them (e.g. by u sing ensemble statistics, instead of the linearized model dynamics, to derive covariances). The problem is further c omplicated, however, by dynamical balances, such as quasi- or semigeostrophic theory, which are themselves only approximations of the true dynamics. Traditionally, balances have been externally enforced after data insertion by reinitializing the analyzed fields. 4D schemes should not require this extra step, since they seek a dynamically co nsistent optimal estimate.

We investigate the representation of balance within different approximations to the nonlinear Kalman Filter, using very simple models of balanced dynamics. Basic experiments with different balance and assimilation parameters il lustrate the issues inherent in the problem of data assimilation for motion with multiple timescales, and some possi ble balance modifications to the assimilation scheme are discussed.

Simulating the Dynamics of Volcanic Columns: a New Challange in Volcanology

Augusto Neri and Tomaso Esposti Ongaro
Istituto Nazionale di Geofisica e Vulcanologia
Centro per la Modellistica Fisica e Pericolosità dei
Processi Vulcanici
Via della Faggiola 32, 56126 Pisa, Italia

Since the middle of the 70s volcanologists have successfully tried to describe the origin of volcanic deposits and complexities of volcanic eruptions on the basis of physical transport laws. First, simple one-dimensional steady-state and homogeneous flow models were used to investigate the different eruptive mechanisms of explosive eruptions as well as the relationships between eruptive style and magmatic conditions. Similar models were developed to describe the fallout of pyroclastic particles from the umbrella region of a buoyant convective column and to study the emplacement and propagation of pyroclastic density currents produced by the collapse of the column. These models were able to capture the main processes controlling the explosive phenomena and still remain a useful tool for a first-order analysis of volcanic sequences.
Based on this fundamental understanding, about 10 years later, the development of the first numerical 2D two-phase flow models indeed started the age of numerical simulation of volcanic processes. New and fundamental features of magma chamber chemical evolution and withdrawal, country rock deformation, magma ascent dynamics, and pyroclastic dispersal into the atmosphere and along the volcano slopes were predicted and compared with direct observations. Despite a large number of limitations, it was shortly clear the added value of this new generation of models.
Nowadays, at the beginning of the third millennium, the development of transient, 3D, multiphase flow models using state-of-the-art formulations of the underlying physics, new-generation experimental data, and high-performance numerical techniques, represents a new opportunity and challange for modern volcanology. In the coming decades, these models will likely contribute to the solution of unresolved problems of the physics of explosive eruptions as well as to a more accurate assessment of their hazard. However, such an opportunity appears to be strictly tied to our capacity to validate the physico-mathematical models developed. In turn, this capacity will mostly depend on the production of reliable transport and constitutive equations of the magmatic mixture through ad hoc laboratory experiments as well as on the collection of accurate quantitative measurements of the ongoing eruptive phenomena.

Flow-induced morphological instability in mushy layers with applications to sea ice

Jerome Neufeld and John Wettlaufer

Department of Geology and Geophysics
Yale University
New Haven, CT, 06511

The effect of oceanic flows on the morphology of the ice-ocean interface is investigated using an analog laboratory system; trans-eutectic ammonium chloride solution. The solution is solidified within a flume, which generates a laminar flow over the growing mushy layer. On a scale much larger than the dendrite spacing, corrugations in the mush-liquid boundary may grow due to the coupling of Bernoulli suction and flow within the partially frozen matrix. The instability is quantified by imaging the morphology of the evolving interface as a function of flow speed and solidification rate, and is then compared with a linear stability analysis. An experimental apparatus designed to test this theory and recent results are presented.

Thermal field of a coupled ocean-atmosphere system: A conceptual model

Hsien-Wang Ou (LDEO of Columbia University)

The paper continues the author's effort to construct a deductive theory of a coupled ocean-atmosphere system forced by the solar insolation. Ou (2001) has determined the global mean fields, which provide the necessary constraints for the present derivation of the meridional thermal field. The model closure invokes MEP (Maximized Entropy Production), a thermodynamics principle widely used in turbulence and climate theories, and whose support is further strengthened by recent developments.

Extending laboratory results, both ocean and atmosphere are first reduced to two thermal masses, with their boundaries aligned at the ocean surface. Subjected to obvious physical constraints, a robust solution is then found, characterized by an ice-free ocean, near-freezing cold masses, mid-latitude fronts, and comparable ocean and atmosphere heat transports. The presence of polar continents however sharply reduces the ocean heat transport beyond the tropics, but leaves the thermal field largely unchanged.

The model system, while greatly reduced, is nonetheless consistent with the large-scale organization of the observed thermal field. And given the limitation of the model approximation, the solution is quite sensible, whose robustness is a direct consequence of MEP. The model results reinforce the premise of energy-balance models that the surface temperature field is largely controlled by thermodynamics, independent of the explicit dynamics.

New estimates for the westward phase propagation of Rossby waves

The classical theory of low frequency planetary waves provides an analytic estimate for the phase speed of Rossby waves in a nearly non-divergent flow on the β-plane by assuming the phase speed and β are both small. Recent observations of the westward propagation of low frequency Sea Surface Height crests/troughs made in the 1990's by the AVHRR altimeter aboard the Topex/Poseidon satellite were interpreted as surface manifestations of westward propagating Rossby waves in the thermocline. Much to the surprise of the Physical Oceanography community, despite the wide range of phase speeds in different times/locations, the observed phase speed always exceeds the theoretical estimates of Rossby waves in mid-latitudes by a factor of 2-4! Since the publication of this observational discovery many modifications of the classical theory were suggested, mainly by including factors that were neglected in the original theory (e.g. horizontal density variations). This talk will report on a recent numerical solution of the eigenvalue problem of low frequency linear waves in a zonal channel on the rotating sphere. The numerically found phase speeds in spherical coordinates are indistinguishable from the classical expression on the β-plane for low zonal wavenumber (i.e. O(10)) and for barotropic cases where the phase speed of gravity waves (i.e. gH where g is gravity and H is the mean thickness of the fluid) is very fast. However, for equivalent-barotropic cases such as those relevant to the Topex/Poseidon observations, where the phase speed of gravity waves is reduced by several orders of magnitudes the gap between the analytic expression on the β-plane and the numerically found phase speeds on the sphere differ by a factor of 2-4.

The source of the difference can be traced by developing a parallel, nonlinear, eigenvalue theory for the phase speed of low frequency waves on the β-plane and on the sphere. We have identified 4 possible sources of error on the β-plane. 1) The geometric error due to the inconsistent expansion of the $\sin(\phi)$ function of the Coriolis term to first order in $\phi - \phi_0$ while keeping the $\cos(\phi)$ function of the metric terms at zero order (i.e. the East-West distance does not change along the North-South coordinate). 2) The violation of Angular Momentum conservation on the β-plane. 3) The assumption of the flow's near non -divergence (also known as the rigid lid approximation). 4) The linearity of the phase speed in the eigenvalue problem in the classical theory. Each of these sources of error affects the error in different circumstances. The geometric error plays a surprising small role in the error. The violation of Angular Momentum conservation on the β-plane has a significant effect on the linear waves' phase speed only in the presence of a mean zonal flow or for very high zonal wavenumbers. The assumption of near non-divergence and the linearity of the (small) phase speed in the eigenvalue problem are related and affect the resulting phase speed for low gravity wave phase speed (i.e. when gH is replaced by g'H', where g' is the reduced gravity and H' is the reduced fluid thickness).

An analysis of the meridional structure of the corresponding eigenfunctions bolster the role played by the violation on Angular Momentum conservation on the β-plane. While the height and meridional velocity eigenfunctions are correctly reproduced by the analytic expressions, the zonal velocity component is in significant error. The only physical quantity that differentiates between the meridional and zonal velocity components is the Angular Momentum.

Effects of spatio-temporal variability of upwelling events on primary productivity.

C. Pasquero, A. Provenzale, A. Bracco

Simple empirical ecological models are coupled to a fluid dynamical model of geostrophic turbulence to explore the effects of advection on the dynamics of the ecosystem, and in particular on primary productivity. The effects of the spatio-temporal scales of the upwelling events that provide the nutrient supply for the planktonic growth are explored. It is found that the variability significantly increases primary productivity in a large range of parameters. Results indicate that any process that increases the average surface area of frontal regions (defined as regions of large nutrient gradients) greatly modifies the ecosystem response to the nutrient input. Effects on the average concentration of nutrients are also explored.

The advection-reaction equations of the ecosystem model are solved in a semi-Lagrangian framework, that allows for a large number of experiments for different configurations of the biological model at low computational costs; the method also allows the control of the diffusivity and does not present the problems common to the integration of evolution equations for positive-definite quantities.

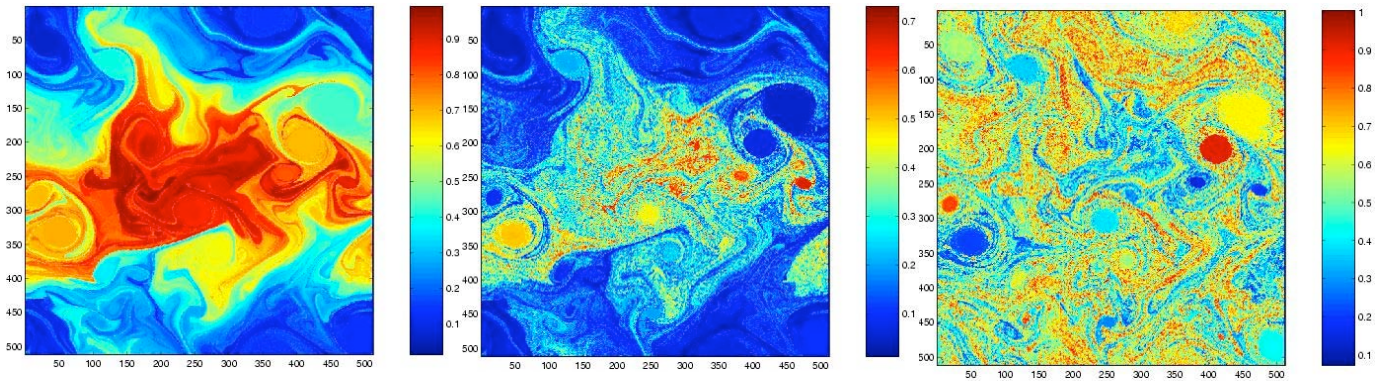

Figure: from left to right, concentration of nutrients, phytoplankton, and zooplankton in the horizontal model domain of size (256Kmx256Km). The system is in a statistically stationary state with upwelling occurring at large scales.

Modeling and Simulation of Hazardous Geophysical Mass Flows Using the TITAN toolset

A. K. Patra, M.F. Sheridan, E. B. Pitman, M. Bursik,
C. Renschler, C. Nichita, B. Yu, A. C. Bauer and K. Dalbey
University at Buffalo, Buffalo, NY 14260

April 15, 2004

High quality computational tools are indispensable for hazard assessment and planning from rapid flow of geophysical masses. The complexity of the physics involved in such events has often led to highly simplistic or empirical/ heuristic models being used. In recent years, first principles based modeling of such flows has been enabled by the use of high performance computing and new techniques for constructing accurate numerical solutions to nonlinear hyperbolic partial differential equations. We will describe in this talk the TITAN toolset developed over the last few years for modeling rapid flows of geophysical masses over natural terrain. Highlights of the TITAN toolset are the use of depth averaged models of the conservation laws and parallel adaptive grid solvers using classical finite volume adaptive grid Godunov solvers and the more recently developed discontinuous Galerkin methodologies. The code is integrated with geographical information systems to obtain terrain/cultural data for simulating flows on natural terrain and displaying their hazard potential. We will discuss in this paper a number issues relating the ability of the simulation in accurately predicting flow paths and runouts for a number of typical flows of interest. In particular, we will explore the model's ability to correctly predict a number of laboratory scale and real flows.

Simulation of Tropical Precipitation using the Weak Temperature Gradient Approximation applied to the Goddard Cumulus Ensemble Model

C. L. Perez, A. H. Sobel and G. Gu

Tropical precipitation due to deep convection is often simulated in models by specifying that convection is present when the atmospheric vertical velocity is above a critical value. This approach neglects the fact the presence of deep tropical convection is a result of heating and is concurrent with and not caused by strong upward drafts. We apply the Weak Temperature Gradient (WTG) approximation to the Goddard Cumulus Ensemble (GCE) model in order to resolve the issues pertaining to this discrepancy.

The WTG approximation is based on observational evidence that shows horizontal temperature and density gradients are small in the tropical atmosphere. Therefore, heating in a column is balanced by the vertical advection of potential temperature. Thus, we can diagnose the model vertical velocity using the heating and static stability profiles which represent the state of the atmosphere as convecting or otherwise.

In this study, we are testing the sensitivity of the modified GCE model precipitation to changes in sea surface temperature and zonal mean wind. We are assessing the robustness of the results with respect to choice of the WTG approximation's base relaxation scheme and with regard to the background temperature profile to which the temperature is relaxed. Results so far indicate that the modeled rainfall is extremely sensitive to SST in a nonlinear manner.

Use of data and coupled modeling of ENSO to detect processes that are not detectable in forced models

Claire Perigaud(*) and Jean-Philippe Boulanger (**)

(* CALTECH/Jet Propulsion Laboratory, Pasadena, CA91109;
818-354-8203; e-mail: cp@pacific.jpl.nasa.gov;

** Laboratoire d'Oceanographie Dynamique et de Climatologie, Paris, France; e-mail: jpb@lodyc.jussieu.fr)

Several examples of processes are identified for having a key impact on the seasonal-to-interannual climate variations simulated by a coupled model of El Nino and a negligible impact when simulated by the model in ocean-forced or atmosphere-forced experiments. Thus, processes like the reflection of waves at the eastern or western boundaries of the ocean or like the driving of the ocean by the off-equatorial wind or by the meridional component of the wind have an impact on the 1980-to-2000 time series of the Nino3 index which is smaller than 0.5 Degree K in forced model simulations. By contrast, canceling any one of these processes during coupled simulations has an impact at least as large as 2 Degree K. Experiments are then designed to understand what role is played by each of these processes in reality. Thus, twenty-year long experiments are performed where the 1980-to-2000 variations of the so-far neglected process are prescribed while every other oceanic and atmospheric variable is being computed by the model equations. By contrast with the data-free fully coupled experiments that drift away from reality in a few months after the model initialization, the use of data to prescribe the so-far neglected process allows to simulate climate anomalies that are in good agreement with the reality observed during 1980-2000. These results illustrate that it is not because of model error growth that coupled simulations diverge from reality, but because the coupling between the ocean and the atmosphere allows processes of little importance in amplitude to play a role in setting up the phase of the system. This conclusion is also consistant with results in paleoclimate that show how the Milankovitch forcing found too weak to explain the drastic amplitude of past climate changes may have played a key role in the phasing of the climate shifts.

Convective entrainment in the tropical tropopause

Frank Robinson
francis.robinson@yale.edu

ABSTRACT

The energy budget near the tropical tropopause is important, because the temperature in that region is thought to control stratospheric water vapor and/or the prevalence of thin cirrus clouds. Both of these affect climate. Radiative transfer calculations indicate that a balance between radiative and convective energy transport is not actually achieved until some point above the cold point (temperature minimum at the top of the troposphere). Observations indicate that temperatures near the tropopause level decrease during convective episodes, but it is not certain whether the observed cooling is due to convective, radiative or adiabatic effects. By using the Weather Research and Forecasting (WRF) model, we are attempting to shed light on this important topic. The sensitivity of convection in the tropical tropopause to vertical grid resolution, geometric dimensions (2D vs 3D) and sub-grid scale turbulence parameterization will be discussed.

Dynamics of the Ancient Carbon Cycle

Daniel H. Rothman
Department of Earth, Atmospheric, and Planetary Sciences
Massachusetts Institute of Technology
Cambridge, MA 02139

Long-term changes in the Earth's carbon cycle are encoded in the isotopic composition of carbon buried in ancient sediments. Extraordinarily large fluctuations in this signal occur in the geologic era preceding the first great diversification of animal life. Analysis of the geochemical records and construction of a simple model indicate that these large fluctuations also precede a major dynamical transition, from a carbon cycle evolving dynamically, far from steady state, to a carbon cycle evolving quasistatically, from one steady state to another. We suggest that this transition reflects a fundamental reorganization of the Earth's biogeochemical cycles.

A Unified Theory of Small Froude Number and Small Rossby Number Balance

Simal Saujani, Theodore G. Shepherd

Balance is a central theme in geophysical fluid dynamics. The atmosphere displays both vortical and inertia-gravity wave motion. However, observations suggest that some of this motion may be considered as noise. A balanced theory of atmospheric motion would propose relationships between the dynamic variables that eliminate or minimize this noise, thus providing a clearer picture of the physics.

Classically, there are two approaches corresponding to two distinct balance regimes. The small Rossby number limit (Charney, 1948) corresponds to a rapidly rotating flow and, as is well known, yields the quasi-geostrophic equations. The small Froude number limit (Charney, 1963) corresponds to a strongly stratified flow and was originally developed for the tropics, where the Rossby number is unbounded. The derivations of these two models are heuristic and completely independent. However, understanding balance as a time scale separation in the dynamics, these models are succinctly realized as special cases of a more general balanced theory.

This is clear with the shallow water f-plane equations. The equatorial region is significantly more complicated; defining balance in terms of a single time scale separation parameter is apparently not so useful. This is interesting since ultimately it is balanced equations uniformly valid on the sphere that we would like. Nevertheless, the idea is a valuable one and we can extend the f-plane results to the equatorial β-plane.

Multifractal Predictability in Geophysics

Daniel SCHERTZER[1] and Shaun LOVEJOY[2]

[1]CEREVE, Ecole Nationale des Ponts et Chaussées, (schertze@cereve.enpc.fr) and Meteo-France, Paris.

[2] Physics dept., McGill U. , Montréal

Time complexity is associated with sensitive dependence to initial conditions and severe intrinsic predictability limits, in particular the 'butterfly effect' paradigm: an exponential error growth and a corresponding characteristic predictability time. This was believed to be the universal long-time asymptotic predictability limits of complex systems.

However, turbulence and geophysics are complex both in space and time and have rather different predictability limits: a limited uncertainty on initial and/or boundary conditions over a given subrange of time and space scales grows across the scales and there is no characteristic predictability time. We argued that complexity in space implies strong limitations on the applicability of the Multiplicative Ergodic Theorem (MET) and of the Liouville equation.

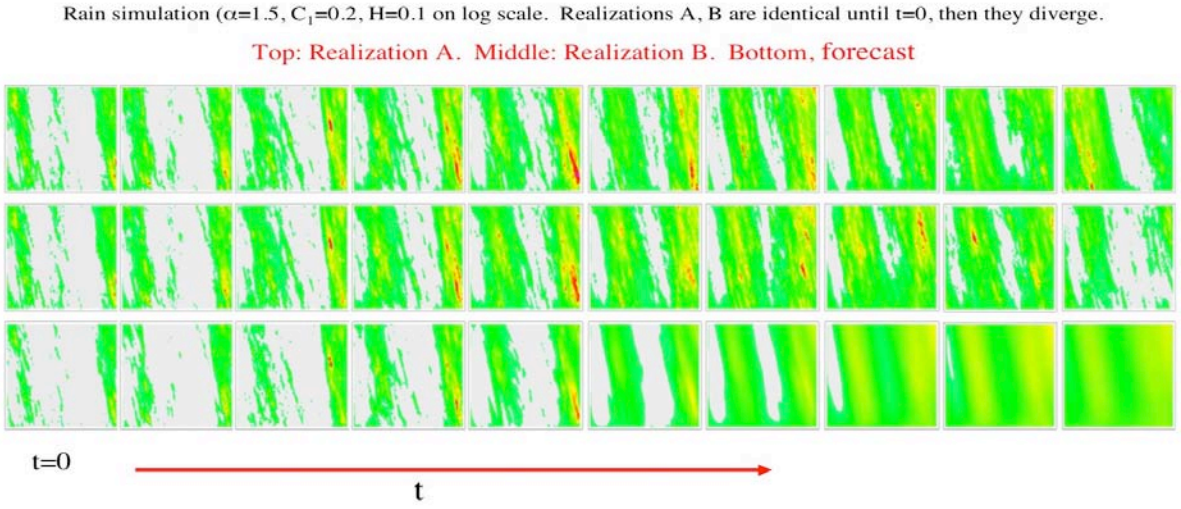

Fig. 1 a-c [Schertzer and Lovejoy, Physica A, in press]: The top two rows (a-b) show successive snap shots of two multifractal simulations that are identical up until time t=0, when their fluxes at small scales becomes step by step independent due the sudden independence of the cascade subgenerators at that time. Most of the difference between the two realizations is concentrated in a few "hot spots". The bottom row (c) shows a forecast based on the "memory" of the evolution up to t=0 of (a), i.e. has the same stochastic subgenerator up until time t=0, then defined in a deterministic manner to preserve the mean of the flux. Note the rapid disappearance of small scale structures.

The relative symmetry between time and space yields scaling (i.e. power-law) decays of the predictability, as confirmed by homogeneous turbulence phenomenology and statistical closure models. Unfortunately, the quasi-normal framework of these models prevents them from dealing

with intermittency: the “bursts” of the energy fluxes through scales, as well as those of information loss.

We show that multifractals offer a very convenient framework to quantify the predictability of space-time complex systems with the help of an infinite hierarchy of exponents. Furthermore, this hierarchy is defined in a straightforward manner for a large class of space-time multifractal processes. We also show that the corresponding scaling function can be used to empirically quantify the predictability of geosystems, as well the performance of forecast procedures. In particular, this readily explains the recent empirical evidence that stochastic subgrid parametrizations do better than deterministic ones.

These results will be illustrated with the help of various numerical simulations, e.g. Fig1, where $t_i=i\,\tau$, i=3,6,..27 (τ being the eddy turn-over time of the smallest structures), the resolution is 256x256 in space, universal parameters are $\alpha=1.5$, $C_1=0.2$, H=0.1 (close to those of rain), color scale is a logarithmic and the anisotropy of space-time is characterized by the dynamical exponent $H_t=2/3$.

Extending the Diagnosis of the Climate of the 20th Century to Coupled GCMs

Edwin K. Schneider
George Mason University/COLA

Forcing ensembles of AGCM simulations with the evolution of the observed 20th century SST, as has been done so far in the C20C project, is a necessary first step to a complete diagnosis of the 20th century climate variability. This step finds the atmospheric circulation feedback to the observed SST evolution. However, since the SST is forced by the atmosphere, diagnosis of the atmospheric feedback alone gives an incomplete and sometimes misleading picture of cause and effect.

According to current theory, a more complete understanding can be reached if the assumed \223external\224 forcing of the SST is atmospheric noise, which produces SST variability in the presence of feedbacks between the atmosphere and ocean. A method is described to extend and apply this type of diagnosis in the context of state of the art coupled GCMs. This involves:

1) Determination of evolution of atmospheric noise for the 20th century using the SST forced ensembles and reanalysis.
2) Determination of the evolution of oceanic internally generated 20th century SST noise using analogous techniques.
3) Forcing of the (noise-free) Coupled Ensemble GCM with the observed atmospheric and oceanic noise evolution.

Self-organization of the atmospheric macroturbulence to critical states of weak nonlinearity

Tapio Schneider

If baroclinic eddies are efficient enough to influence the thermal stratification of an atmosphere, they adjust the stratification such that nonlinear eddy-eddy interactions of the atmospheric macroturbulence are weak. States of strong nonlinear eddy-eddy interactions and accompanying inverse energy cascades appear not to be attainable in the atmosphere, notwithstanding their attainability (and prominence) in quasigeostrophic models.

Simulations with an idealized general circulation model over wide range of climates show that the supercriticality, or nonlinearity, of atmospheric flows initially increases with increasing baroclinicity but levels off and remains nearly constant if the baroclinicity is increased beyond a critical value. The critical value of the baroclinicity at which the supercriticality reaches saturation is the value at which baroclinic eddies begin to exert a significant influence on the thermal stratification. For baroclinicities less than the critical value, the stratification is set by convection; for baroclinicities greater than the critical value, the stratification is set by baroclinic eddies. Turbulent fluxes, for example, of heat and momentum exhibit a phase transition at the critical value, with different power laws for the scaling of the fluxes on either side of the phase transition. In the phase in which baroclinic eddies set the stratification, one obtains a scaling theory for turbulent fluxes of heat and momentum by using the fact that eddy-eddy interactions are weakly nonlinear, paired with considerations of the energy cycle of the atmospheric circulation. The scaling theory is consistent with the results of simulations with the idealized GCM.

The Evolution of Fault Populations with Brittle Strain

C. H. Scholz[1], B. E. Shaw[1], C. Spyropoulos[2,3]

Three types of fault or joint populations are observed in nature, power law, exponential, and evenly spaced system sized cracks in which the spacing is proportional to the brittle layer thickness. We developed a spring-block model simulating the stretching of a brittle layer on a ductile substrate, in which the blocks may fracture, following a slip-weakening criterion. At low strain, the density of active cracks in the model first increases linearly with strain, but then begins rolling off to a maximum, after which it gradually decreases, eventually reaching a constant value at high strain. In the first, linearly increasing regime, the crack population size distribution was exponential. This gradually changes to a power law distribution as the peak is approached, then as the crack density decreases, gradually evolves to a exponential distribution of the longest cracks. At very high strain where the crack density became constant, the active cracks were long and approximately evenly spaced at a distance scaling with the brittle layer thickness and the strength slip-weakening length. This same behavior was reproduced in a physical model, in which a clay layer was stretched on a rubber sheet. We interpret the results in the following way. The early exponential distribution simply reflected the system disorder in a dilute, non-interacting crack population. As crack density and lengths increase, the cracks begin to interact, resulting in a power law regime. As strain increases further, interactions dominate, resulting in both a reduction of nucleation and extensive crack pinning from stress shadowing, and a reduction of cracks by coalescence. This distorts the power law into a exponential. Finally the system saturates with cracks spaced by their stress shadow distance, which scales with layer thickness. Observation of natural crack populations agree with these results: power law fault distributions are observed at 1-2% brittle strain and exponential fault distribution are observed on the flanks of the East Pacific Rise where the brittle strains are 10-15%. Evenly spaced crack distributions have been observed only for joints, in which their spacing is proportional to layer thickness. A transect across the rift in Djibouti showed that fault density increased approximately linearly for the first 4% brittle strain, where the faults grew with a constant displacement/length ratio, indicating few interactions. By 8% strain, the fault density was decreasing and the strain was being accommodated by increasing D/L ratios, indicating that most faults were pinned or coalescing. The length distribution for faults at <8% strain was power law, and above 8%, exponential, in agreement with the models.

1. Lamont-Doherty Earth Observatory, Columbia University, Palisades, NY
2. Department of Allied Physics and Applied Mathematics, Columbia Univ., NY, NY.
3 Presently at: EXXON-Mobil Downstream Research, Houston, Texas.

Wavelet Maxima Curves for the Analysis of Surface Latent Heat Flux Data

G. Cervone,D. Napoletani, M. Kafatos, R.P. Singh
School of Computational Sciences
George Mason University
Fairfax, VA 20030

Significant changes in land, ocean and atmospheric parameters have been observed prior to earthquake events. Recently, Surface Latent Heat Flux (SLHF) has been found to exhibit anomalous behavior prior to large coastal earthquakes. The observed anomalies suggest the existence of interaction between the lithosphere and the atmosphere, and have opened up new possibilities to the use of remote sensing observations to identify and study earthquake precursors.

The yearly time series of the SLHF contains a large number of maxima peaks, several of which are more than 1 or 2 times above the standard deviation. These peaks are due to atmospheric phenomena, earthquakes, or ocean disturbances, and therefore the main challenging task is to identify the SLHF peaks that are precursors of an impending earthquake.

The SLHF is a parameter directly related to the evaporation of water on the surface. SLHF is particularly affected by changes in temperature over the land and over the oceans. The change in surface temperature can be due to atmospheric perturbations, such as strong winds, precipitation, intense cloud cover, or due to geological phenomena.

In this paper, we present a methodology based on wavelet transformations to find singularities in the data. A one dimensional wavelet transformation has been performed over one year of daily SLHF data using the second derivative of Gaussian as mother wavelet. The local maxima of the wavelet transform are computed at different scales, and interpolated along the scale/time plane to generate *maxima curves.* Each maxima curve corresponds to an anomalous peak.

The SLHF shows numerous peaks over the year which may or may not be associated with an impending earthquake. In the present methodology , we have considered only the peaks corresponding to maxima curves which propagate from finer to coarser scales and with a minimum length above a predetermined threshold. Additionally least significant peaks are filtered out by discarding those with magnitude below the average value computed using data for several previous years for the same time of the year.

The wavelet based method has also been found to be an effective technique to filter out peaks caused by small high frequency variations (causing very short maxima curves) and peaks caused by the seasonal trend of the SLHF, since maxima curves do not have to propagate to the coarsest scale.

The use of the present methodology will be demonstrated using SLHF data associated with the occurrence of several large coastal earthquakes for giving early warning information.

A simple model of SST hot spots, and coupled dynamics of tropical intraseasonal oscillations

Adam H. Sobel*
Columbia University
New York, NY

Hezi Gildor
Weizmann Institute of Science
Rehovot, Israel

Eric Maloney
Oregon State University
Corvallis, OR

Abstract

I will start by presenting a very simple single-column model for the interaction between deep convection, cloud-radiative feedbacks, surface fluxes, and thermal ocean coupling in a single column near the equator. For plausible parameters, steady solutions of this model are unstable to time-periodic recharge-discharge oscillations. The resulting disturbances have intraseasonal periods and some features in common with the observed intraseasonal oscillation (ISO). When the model is placed in a marginally stable regime and forced with an imposed atmospheric oscillation, the amplitude of the resulting oscillations has a non-monotonic dependence on ocean mixed layer depth. The maximum response occurs around depths of 10-20 meters, with smaller responses at both larger and smaller mixed layer depths.

I will present simulations designed to test this result using a general circulation model (GCM), coupled to a slab ocean model in which the (fixed) mixed layer depth is varied. The non-monotonic dependence on mixed layer depth predicted by the simple model is indeed found in the ISO simulated by the GCM.

I will argue that the mechanism responsible may explain the ISO amplitude minimum which is found in the maritime continent region. The results also show that a nonlinear form of surface flux convection feedback (WISHE), as well as the recharge-discharge mechanism of the simple model, is important in the GCM.

*Full address: Department of Applied Physics and Applied Mathematics, Columbia University, 500 West 120th St., Rm. 217, New York, NY 10027. E-mail: ahs129@columbia.edu

Towards an integrated theory of geochemistry and geodynamics

Marc Spiegelman

Depts. of Applied Physics and Applied Math & Earth and Environmental Sciences
Columbia University, New York, NY, mspieg@ldeo.columbia.edu

The compositional variability of lavas, melt inclusions and residues sampled from the Earth's mantle is a primary observation constraining dynamic processes at depth. Nevertheless, understanding the dynamic implications of these observations remains a challenge because chemical variability results from at least two scales of processes. At the largest scale, mantle convection produces a chaotic stirring problem that stretches and folds source variations. However, given the extremely small diffusivity of chemical constituents in the solid state, this process neither mixes, fractionates or homogenizes the source. These processes occur at a much smaller scale in the presence of melting and melt transport. The question remains as to how this second scale of process affects chemical variability and ultimately the distributions of composition observed at the surface.

While it might be expected that melt transport leads to enhanced mixing and a reduction in chemical variability, both field evidence and recent calculations suggest that melt transport processes can preserve large chemical variations on small length scales and may actually enhance variability through the development of a channelized melt transport network.

We review observations of chemical variability in lavas and melt inclusions from mid-ocean ridges and show that these systems display large trace-element concentration variability with little obvious spatial correlation on all scales from 1000 km of ridge down to the hand-sample scale measured in melt inclusions. While some of this variability is due to source variations, we suggest that a large component could be the consequence of magma transport in channelized systems. We review field evidence from ophiolites that suggests that "replacive dunites" are a likely candidate for such channels and we describe numerical models that explore channel formation and localization by reactive magma transport.

Given these physical models for channel formation, we explore the chemical consequences of these processes. We show that channelized flow can produce orders of magnitude variation in the concentrations of highly incompatible elements, even for idealized systems with a homogeneous source, constant bulk partition coefficients and equilibrium transport. Most importantly, the full range of variability is found in each channel due to advection of highly depleted melts from the inter-channel regions into the edges of the channels. As these channels may be spaced on scales of 1–100 m in the mantle, this mechanism allows highly variable melts to be delivered to the Moho on very small length scales. We show that the chemical variation produced in the models is consistent with that seen in melt inclusion suites, lavas and residual mantle peridotites dredged from the ridges and sampled in ophiolites.We discuss new models that include the effects of spatially varying partition coefficients and consequences for U-series disequilibrium.

Sedimentary fingerprints and consequences of asymmetric flow fields surrounding isolated topography

Robert Turnewitsch	*Southampton Oceanography Centre, European Way, Southampton SO14 3ZH, United Kingdom; rxt@soc.soton.ac.uk*
Jean-Louis Reyss	*Laboratoire des Sciences du Climat et de l'Environnement, France*
David C. Chapman	*Woods Hole Oceanographic Institution, USA*
John Thomson	*Southampton Oceanography Centre, United Kingdom*
Richard S. Lampitt	*Southampton Oceanography Centre, United Kingdom*

Kilometer-scale topographic seafloor elevations of comparable breadth and width like abyssal hills, knolls, and seamounts are ubiquitous features on the global oceanic seafloor. Physical oceanographic modeling and field studies have shown that such seafloor elevations are surrounded by complex flow fields. Asymmetric flow fields, reversed flow and closed streamlines around the topographic feature (Taylor caps), and resonantly amplified tidal currents around the seamount rim potentially control near-bottom particle dynamics, particle deposition at the seafloor and, consequently, the formation of the sedimentary record.

We combine numerical modeling and field data to study how such topographically controlled flow-field features are reflected in the sedimentary record. Sediment deposition on a topographically isolated abyssal knoll (height: 900 m) on the Porcupine Abyssal Plain in the Northeast Atlantic (water depth above the abyssal plain: 4850 m) was studied, (1) by comparing the spatial distribution of ^{210}Pb fluxes, calculated from inventories of sedimentary excess ^{210}Pb, with ^{210}Pb input from the water column as recorded by sediment traps; and (2) by comparing sedimentary grain-size distributions and Zr/Al ratios (an indicator for contents of the heavy mineral zircon) at slope, summit and far-field sites. Given Rossby numbers $\geq$0.23, a fractional seamount height of ~0.2, and the absence of diurnal tides it is concluded that an asymmetric flow field without Taylor cap and without amplified tidal currents around the seamount rim is the principal flow-field feature at this knoll.

The results and conclusions are as follows: (A) Geochemical and grain-size patterns in the sedimentary record largely agree with the predicted pattern of flow intensity around the topographic elevation: with increasing current strength (erosiveness) there is evidence for a growing discrepancy between water column-derived and sediment-derived ^{210}Pb fluxes, and for increasing contents of larger and heavier particles. This suggests that the topographically controlled flow field distorts a homogeneous particle-flux input signal from the ocean interior and results in kilometer-scale differences of the amount and composition of the deposited material. (B) The fact that, at the summit, the sediment-derived ^{210}Pb flux is lower than the water-column-derived ^{210}Pb flux indicates that the passing water is partly advected around *and* partly advected *over* the knoll. This agrees well with the model results. (C) The orientation of the sedimentary pattern indicates that at least during the past 100 years (~5 ^{210}Pb half lives) northward currents prevailed within the lowest ~1000 m of the water column on the Porcupine Abyssal Plain. The fact that the modelled spatial current-velocity distribution shows a better match with sedimentary velocity (erosiveness) proxies at higher than at lower inflow velocities suggests that mean far-field current velocities might have been higher in at least the past 100 years as compared to today.

More comprehensive studies of this kind could provide information on paleo-changes of the orientation and current velocity of flow fields in the deep ocean. At the end of the presentation we will briefly speculate about possible conclusions for latitudinal gradients and changes throughout Earth history of the intensity of the asymmetries, and consequences for ecosystem structure.

Stability of Viscous-Plastic Sea Ice Rheology: 1-D Approximation Method

JINRO UKITA
Lamont-Doherty Earth Observatory, Columbia University
61 Rt 9W, Palisades, NY 10964, USA
E-mail: jukita@ldeo.columbia.edu

JUN YU and GUANGHUI WANG
Department of Mathematics and Statistics, University of Vermont
16 Colchester Ave, Burlington, VT 05401, USA
E-mail: Jun.Yu@uvm.edu , E-mail: gwang@emba.uvm.edu

We present the results from stability analysis on viscous-plastic sea ice formulation. In recent years the stability of this formulation, which is a standard component in many of the present-day sea-ice/atmosphere/ocean coupled models, has become a subject of controversy. In the context of sea-ice dynamics, an issue of stability arises due to a discontinuity in the stress state associated with yielding, thus to the extent inherent to the plastic formulation. In this study we introduce an approximation method, by which this discontinuity is treated as a limit for a sequence of continuous and well-behaved constitutive relations. This method in turn gives both an analytically and numerically stable solution to the problem. In particular we shall show that for the 1-D case the approximate model is stable in the limiting sense and further eliminates a need for an artificial diffusion term from the sea-ice model. We shall also discuss the extension of the approximation method to the 2-D framework.

Volcanic forcing improves AOGCM scaling performance

DmitrVyushin (vyushin@atmosp.physics.utoronto.c a)

Recent Global Climate Models simulations of the twentieth century climate, which account for anthropogenic and natural forcings, make it possible to study the origin of long-term correlations found in the observed records. We study ensemble experiments performed with the NCAR PCM for 10 different historical scenarios, "no forcings", "greenhouse gas", "sulphate aerosols", "ozone", "solar", "volcanic forcing" and various combinations, such as "natural", "anthropogenic" and "all forcings". We compare the scaling exponents characterizing the long-term correlations of the observed and simulated model data for 16 representative land stations and 16 sites in the Atlantic Ocean for these scenarios. We find that inclusion of volcanic forcing improves the PCM scaling behavior.

The scenarios containing volcanic forcing better reproduce the observed scaling exponents for the land with exponents about 0.63 independent of the station distance from the nearest ocean. For the Atlantic Ocean, scenarios with the volcanic forcing slightly underestimate the observed persistence exhibiting an average exponent 0.74 instead of 0.85 for reconstructed data.

Numerical simulations of vortical and wave motion in stably stratified turbulence.

Michael Waite and Peter Bartello, McGill University

Observations of the atmospheric mesoscale and oceanic submesoscale, where stable density stratification is strong but rotation is weak, have a certain universality: energy spectra, for instance, are often found to be relatively independent of location and season. Different theories have been proposed to account for these observations; however, the underlying physics remain controversial. This issue has implications for climate research, as the dynamics of these intermediate scales have effects on the large-scale flow which must be parameterized in GCMs. An important feature of stably stratified flows is that they can be decomposed into a vortical component (possessing potential vorticity) and an internal wave component. In the strongly stratified limit, these two modes of motion have very different dynamics. Vortical motion, unlike internal waves, remains fully nonlinear, and its limiting dynamics correspond to decoupled layers of two-dimensional turbulence. In the atmosphere and ocean, the limiting dynamics break down at small scales; the nature of the breakdown, and the dynamics at these scales, remain unclear.

In this talk, we examine stratified turbulence dominated by both vortical and wave motion for a wide range of stratifications. We present numerical simulations of a Boussinesq fluid, in which vortical and wave motion are forced separately at large scales. Stratifications range from weak (nearly isotropic) to strong (the limiting regime). In the vortical case, the vertical decoupling predicted by the limiting equations is observed. The corresponding energy spectra are flat in the vertical wavenumber k_z. The decoupling is shown to break down at a vertical scale of U/N, where U is the RMS velocity and N is the Brunt-Väisälä frequency Wave energy is generated by nonlinear interactions at this scale. At moderate stratifications, the horizontal wavenumber energy spectra are consistent with $k_h^{-5/3}$; however, as N is increased and small-scale turbulence is suppressed, a limiting form of k_h^{-5} is reached. We contrast these findings with wave-forced simulations, and discuss the relation of our numerical results with different theories of wave and vortical motion. The effects of vortical motion on wave dynamics is also addressed.

The entrainment rate of a rotating gravity current.

Mathew Wells & John Wettlaufer
Department of Geology and Geophysics, Yale University, New Haven,CT

A gravity current flowing down a slope entrains surrounding fluid, with the result that the density contrast of the gravity current decreases and the volume increases. This rate of increase in volume is known as the entrainment rate. In a few regions of the oceans there are sites where dense waters flow down continental slopes under the influence of buoyancy and Coriolis forces. As these dense waters sink they entrain surrounding fluid which modify the original water mass properties. If dense enough, these water masses will spread at depth over the base of the worlds oceans, providing the source of deep waters for the thermohaline circulation, often called the global "conveyer belt".

We will present new laboratory experiments of measurements of the entrainment rate of a gravity current as a function of slope and rotation rate. In a finite volume container the outflow from the gravity current will start to build a background stratification and circulation, analogous to the oceanic thermohaline circulation. We will show how the entrainment rates of a rotating gravity current on a slope can be related to the classic Baines & Turner (1968) filling box model, in order to predict the long term stratification and circulation timescales.

Caustic Grain Boundary Melting in Ice

J. S. Wettlaufer[1,2], L. Benatov[2] and L.A. Wilen[1]

Yale University
Department of Geology and Geophysics[1]
Department of Physics[2]
New Haven, CT 06520

The equilibrium state of grain boundaries and the vein-node-trijunction system in polycrystalline materials is fundamental to a broad range of geophysical problems. Hence, a basic understanding of grain boundary melting touches a number of fields. The value of studying the phenomenon in ice is that experimental tests can be designed that exist in thermodynamic equilibrium. The effect of impurities on the grain boundary melting of ice is investigated using modified Derjaguin-Landau-Verwey-Overbeek theory. We calculate the full frequency dependent van der Waals contribution and Coulombic interactions within doped ice grain boundaries. Because the long range contributions are attractive (suppress melting) and the screened Coulomb interactions are repulsive a film forms at high temperature but as the temperature is lowered, depending on the dopant level and surface charge density, an abrupt jump to zero (or small but finite) grain boundary thickness is predicted.

StochAOabstract

Using a simple model, we investigate the occurrence of a dipole in first empirical orthogonal function (EOF) of a stochastically forced atmospheric zonal flow. Such dipoles, commonly referred to as the Arctic Oscillation or the Northern Annular Mode (AO/NAM), have been robustly identified in the observations, and appear to be ubiquitous in modeling studies. Without appealing to fluid dynamical principles, we show that the characteristic dipolar shape of the first EOF is a simple consequence of the existence of a singly-peaked jet whose center moves stochastically about a mean position.

The possibility that the stratosphere might exert significant dynamical influence on the troposphere has recently attracted much attention. In this work we investigate how stratospheric conditions might alter the development of baroclinic instability in the troposphere. Starting from the LC1 paradigm of Thorncroft et al. 1993, we consider the evolution of baroclinic lifecycles resulting from the addition of a stratospheric jet to the LC1 initial condition. The synoptic evolution of the resulting lifecycles is compared to the reference case with no stratospheric jet. The evolution of the stratospherically influenced lifecycles is described, and the tropospheric response is mapped over the space of stratospheric jet parameters. Significant departures from the LC1 paradigm are observed over a large range of stratospheric jet parameters, with synoptic-scale differences to the surface geopotential whose zonal averages in many cases exhibit meridional dipole structures that resemble the Arctic Oscillation.

Statistical Significance Test of Intrinsic Mode Functions

Zhaohua Wu
Center for Ocean-Land-Atmosphere Studies
Calverton, Maryland, USA

ABSTRACT

One of the preliminary tasks of analyzing a data set is to determine whether the data set or its components contain useful information. The task is essentially a binary hypothesis testing problem in which a null hypothesis of pure noise is often pre-proposed. To test against the null hypothesis, the characteristics of noise need to be understood first; and often, these characteristics of noise are pertained to the analysis method that is used.

In this talk, the characteristics of white noise in the Empirical Mode Decomposition method (EMD) are discussed. EMD has successfully revealed empirical facts for a long stream of data of synthetic white noise: (i) the EMD is effectively a dyadic filter, (ii) the Intrinsic Mode Function (IMF) components are all normally distributed, and (iii) the Fourier spectra of the IMF components are all identical and cover the same area on a semi-logarithm period scale. These empirical findings help infer that the product of the energy density of IMF and its corresponding averaged period is a constant and the energy density function satisfies a Chi-squared distribution. The energy density spread functions of the IMF components can then be derived based and these functions are used to design statistical testing methods against white noise for the IMFs. To demonstrate its validity and effectiveness, the EMD method is applied to somewell known geophysical data sets, such as the SOI, NAO Index, and globally averaged surface temperature anomaly

The Ocean and Thermohaline Loops, Stommel Box Models, and Sandström's Theorem

Carl Wunsch
Department of Earth, Atmospheric and Planetary Sciences
Massachusetts Institute of Technology
Cambridge MA 02139
email: cwunsch@mit.edu, fax: 617-253-4464

May 2, 2004

Abstract

A two-box ocean model published by H. Stommel in 1961 has become widely used as an analogue for the behavior of the time-varying climate state of the ocean. This box model is kinematically and dynamically equivalent, however, to the flow in a one-dimensional fluid loop, although with awkward mixing coefficients. More generally, such a loop, when heated and cooled at the same geopotential, provides a simple example of the working of Sandström's Theorem, suggesting that the flow energetics are completely controlled by specification of the supposedly turbulent diffusion coeffients. Here flow intensity can be both increasing and decreasing with growing diffusion. Stress dominates real oceanic flows, and its introduction into the purely thermally driven loop generates oscillations, multiple states, and instabilities at low diffusivity. When salinity (but not mass) forcing and mixed boundary conditions are further introduced, an intricate pattern of response, dependent upon at least five non-dimensional parameters, including the time of onset of salinity forcing, appears. The ability, in a one-dimensional loop, to produce such a rich array of dynamical behaviors, dependent in detail upon the problem paramters, suggests that in the absence of any general results relating one- to three-dimensional fluid flows, identification of the time-dependent behavior of a GCM with that of the one-dimensional loop-Stommel models should be regarded as speculation..

A simple model of aeolian megaripples

Hezi Yizahq
BIDR, Ben Gurion University, Sde Boker Campus 84990, Israel
E-mail address: yiyeh@bgumail.bgu.ac.il

Aeolian sand ripples are a common feature in sandy deserts and on beaches. Standard aeolian ripples have wavelength of a few of tens of cm, and amplitude of a few mm. Sometimes, much larger ripples are observed (see Fig. 1). These latter have been termed in different such as ridges, granule ripples, megaripples or gravel ripples. Aeolian megaripples are composed by a mixture of coarse and fine non-cohesive material; a bimodal distribution of particle sizes is thought to be necessary for large ripple-like bedforms to develop. The coarse grains account for 50-80% of the surface material at the crestal area and for no more than 10-20% of the surface material in the troughs. Megaripples are characterized by an asymmetric profile, with wavelength up to 20 m and amplitude of tens of cm. There is a correlation between the ripple height and the ripple wavelength, with ripple index (the ratio between the wavelength to the height) of approximately 15, and between the megaripple wavelength and the ripple maximum particle size. Field observations indicate that often megaripples have normal ripples superposed on both their windward and lee slopes.

Fig.1: Aeolian megaripples at the Southern Negev in Israel. The megaripples mean wavelength is about 70 cm. Standard sand ripples can be seen in the troughs which had been formed by gentler winds.

Although many models of the dynamics for the formation of standard aeolian ripples are available, the mathematical description of megaripple evolution has received little or no attention. Here, we build on the integro-differential aeolian ripple model proposed by Anderson [1] and recently extended by Yizhaq et al. [2], by including spatial variations of the saltation flux.
The main idea is that the sediment consists of a mixture of sand grains with two different sizes and that the wind is not strong enough to cause the coarse fraction to saltate [3]. The simplified model [4] takes into account both saltation and reptation fluxes in the so-called Exner equation. Spatial variability of saltation flux is due to large enough undulations of the bed. In such cases, the saltation flux can depend on the bed topography such that it decreases at the windward face while increases at the leeward of the ripple. In these latter cases, the spatial variability of the flux of saltating grains, as well as the feedback of the bedform on the sand flux, must be taken into account. The variability of the saltation flux leads to space-time dependence of the number density of impacting grains on a flat surface which makes the problem quite complicate. We focus only on lineraized dynamics, and for simplicity assume that the number density of impacting grains to be constant. It is a

two scales model where spatial variations of the saltation flux dominates at large scales (order of meters) and for long times, while spatial variations of the reptation flux dominates on small scale (order of cms.) and for shorter time scale. Linear stability analysis indicates the presence of two maxima in the growth rate of the unstable modes (see Fig. 2). The gravest mode corresponds to megaripples and the other to ``standard'' aeolian sand ripples. The model predicts that the megaripple wavelength is about several times the mean saltation hop length.

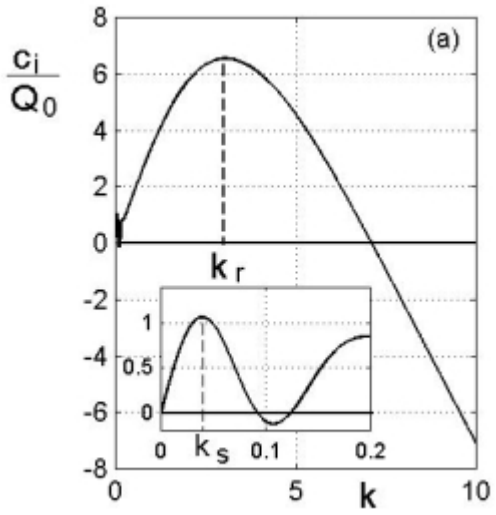

Fig. 2: Linear stability analysis of the model equation indicates the presence of two maxima in the growth rate curves. The first maximum pertains to ripples with wavelength with $\lambda_s = 157\,\mathrm{cm}$ and the second (shown in the inset) to ripples with much a shorter wavelength $\lambda_r = 2.09$ cm.

The proposed model can explain the formation of huge megaripples on Mars [5], where the thin Martian atmosphere greatly increased the saltation length .The model can be extended to include situations where the wind is strong enough to cause saltation of the coarse particles i.e when the wind velocity is above the impact threshold for the coarse grains. For these cases the megaripple wavelength decreases several times in agreement with wind tunnel observations. Provided real values for the various parameters, the model can be used to predict megaripple wavelength and the minimum percent of coarse grains at the surface needed for megaripple formation.
We should keep in mind, however, that the proposed model is only a first step in megaripples modeling and many questions regarding megaripples formation are still remain open.

References:

[1] Anderson, R.S., Sedimentlogy 34 (1987) 943.

[2] Yizhaq, H., N.J. Balmforth, A. Provenzale. Blown by wind: Nonlinear dynamics of aeolian sand ripples. Physica D (2004), to appear in Physica D.

[3] Ellwood J.M., et al. Small scale aeolian bedforms. Journal of Sedimentary Petrology (1975), 45, 2, 554-561.

[4] Yizhaq, H., A simple model of aeolian megaripples (2004). To appear in Physica A.

[5] Wilson, S.A. et al. Large aeolian ripples: Extrapolations from earth to mars. Lunar and Planetary Science XXXIV (2003). 1862.pdf.

THE DYNAMICS OF HYDROUS COLD PLUMES SEEN THROUGH ONE BILLION TRACERS

David A. Yuen (1), Taras V. Gerya(2), Maxwell Rudolph (3), Allison Capel (1), and Erik O.D. Sevre (1)

1. Department of Geology and Geophysics and Minnesota Supercomputing Institute, University of Minnesota, Minneapolis, MN 55455

2. Geology Institute Sonneggstrasse 5, E.T.H., CH-8092, Zurich, Switzerland

3. Department of Geology, Oberlin College, Oberlin, OH 44074

Recently the role of water in geodynamics is receiving greater and greater attention, driven by laboratory experiments, seismic analysis and numerical modeling. Introducing water into the dynamical models changes the nature of the equations to a complex system characterized by multiple components with many different intrinsic scales. We have modeled the dynamics of hydrous plume development above subducting slabs. Our 2-D model incorporates the effects of thermal-chemical buoyancy as well as the combined effects of both hydration and melting. We have used up to ONE BILLION tracers to delineate the evolution of the lithological, rheological and deformation structure of subduction zone with resolution down to between 10 and 50 meters. Tracers are integrated simultaneously with a Lagrangian energy equation and the solution is interpolated back to an Eulerian system for the solution of the thermal-chemical momentum equation. The rheologies of the different components are explicitly included. We have found the following interesting result.In contrast to common dogmatic thought that hot rising mantle flows prevail in the mantle wedge above the subducting slab our results suggest that partially molten hydrated upwellings (WET COLD PLUMES) in the mantle wedge are characterized by a colder thermal anomaly of 300 to 400 degrees! This rather unique process is produced by the subduction of buoyant crustal rocks and infiltration of aqueous fluids releasing from the slab, particularly due to decomposition of serpentine at depths >100 km. Low viscosity of these silicate bearing fluids under subsolidus conditions results in a rapid upward transport of water from the slab toward the melting front that forms within the mantle wedge. This melting front lies nearly parallel to the slab and is located just a few kilometers atop the slab. Higher viscosity and slower infiltration of hydrous basaltic melts formed above the melting front produces a slab-parallel layer of partially molten peridotite which is the source layer for the unmixed cold plumes transporting magmas of peridotitic origin. Mixed cold plumes responsible for transportation of crustal and mixed magmas starts directly from the slab and consist of hydrated, partially molten both mantle and subducted crustal rocks mixed over hundreds to tens of meter scale. Unmixed and mixed wave-like structures were also observed and they propagate upward along the descending slabs. Both cold plumes and cold waves may have an upward velocity >1 m/year, thus rapidly transporting thousands of cubic kilometers of rocks and magmas. Visualizing one billion tracers is indeed a daunting task and a grand challenge problem. Currently there exists is

no single display device available for unveiling all of the minute details in one fell swoop. In order to address this serious obstacle in visualization , we have developed two solutions for remote visualization and for local visualization. Our remote visualization solution is based on the web, and is a zoomed-in image service (WEB-IS3, available on http://tomo.msi.umn.edu/~max/webis) that requires minimal bandwidth ,while allowing the user to explore our data through time, across many thermo-physical properties, and through different spatial scales. For local visualization, we found it optimal to use 2 bandwidth-intensive, high-resolution display walls for performing parallel visualization in order to best comprehend the causal and temporal dynamics produced by the multiple physical and chemical properties in subduction zone dynamics.

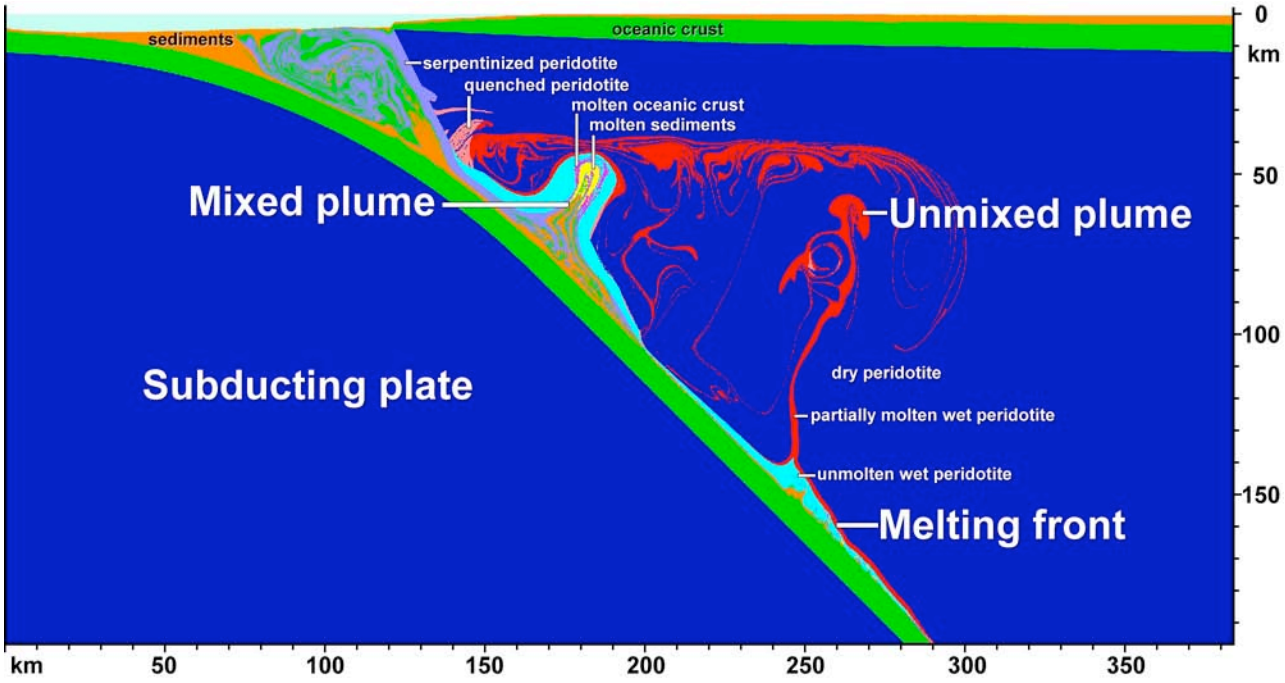

Figure : Results of numerical experiment of the developing mixed and unmixed hydrous cold plumes during oceanic subduction over hundred million tracers were employed in this run. Subduction of 120 million year old oceanic slab is modeled for a rapid subduction speed of 8 cm/a, characteristic of the Japanese subduction zone. We visualize here the multi-component compositional field at a time of 7.8 Myr after the onset of subduction.

Multiscale Trend Analysis: a new approach to studying complex time series

I. Zaliapin, A. Gabrielov, V. Keilis-Borok

Practically every time series emerging in science involves interplay of trends at different scales. Obvious examples are alternations of seismic activation and quiescence, intermittence of warming and cooling of atmosphere and ocean, upward and downward slopes of a landscape, etc. Information on these trends is very important in many problems ranging from classical statistical interpolation of time series to prediction of natural disasters. Powerful Fourier and wavelet analyses are not always convenient since they reflect information on trends only indirectly.

We introduce a new technique, Multiscale Trend Analysis (MTA), for decomposition of time series into a hierarchy of trends at different scales. As a result, a time series $X(t)$ is represented by a tree M_X whose nodes correspond to single trends. The larger is the scale at which the trend is observed, the higher is the corresponding node in the tree. Important advantage of the proposed trend decomposition is that it is very intuitive, allowing field-specific physical interpretation for M_X; this feature can not be overestimated at exploratory stage of data analysis.

We describe and analyze the topological and metric structure of M_X and show that the metric structure is connected in a unique way to the Hurst exponent H of the corresponding self-affine series $X(t)$; it can be used as well to estimate local Hurst exponents $H(t)$. On the contrary, the topological structure of M_X is shown to be super-invariant in the sense that it is universal for fractional Brownian walks with $0 < H < 1$; thus the variations of the topological structure reflect deeper properties of the analyzed processes comparing to fractal dimension.

The correlation analysis of time series is introduced based on the MTA. It is shown to be robust and effective in detecting correlations between non-stationary time series with non-linear long-term trends and observed at irregular non-coincident time grids.

Various applications of the Multiscale Trend Analysis are demonstrated using fractal Brownian motions, and observed data from seismicity, geodynamics, hydrology, biology, and finance.

Role of Compositional Stratification on the Evolution of Planets

S.E. Zaranek, E.M. Parmentier,and L.T. Elkins-Tanton
Brown University, Department of Geological Sciences, Providence, RI 02912

Solid-state thermal convection has frequently been assumed important in understanding planetary thermal evolution. Compositional stratifications, for example the core and the mantle of the planet, are well recognized to have a major influence on planetary structure. However, density variations due to composition in planetary silicate mantles can be large compared to those temperature differences available to drive thermal convection. Not only can the compositional variations be large, but for thermally-activated creep, the rheologically controlled temperature difference that can drives thermal convection can be small.

For moderate sized planets, the energy due to accretion and differentation of the metallic core should be sufficient to melt at least part of the silicate planet, creating a magma ocean. Since the solidus temperature increases with depth more rapidly then the adiabat, solidification of this magma ocean will occur from the bottom up. Liquid-solid chemical fractionation during solidification leads to an unstable density stratification in the initially solidified magma ocean. The late-stage crystallized materials are richer in Fe and incompatible elements such as U, Th and K. Overturn of this initial unstable stratification would lead to a stable compositional stratification. Adiabatic melting resulting from overturn may be a viable mechanism for the production of the earliest crust. The resulting stable compositional configuration would control the subsequent evolution of the planet through the distribution of heat producing elements, isotopic compositions, and compositional controls on density and rheology.

A stable compositional stratification in planetary mantles could also arise from partial melting due to adiabatic decompression as the planet evolves. Therefore, compositional stratification may be important in the thermal evolution of oceanic upper mantle and the formation of subcratonic lithosphere, both of which may be residuals of mantle melting. In general, stable compositional stratification suppresses or delays the onset of thermal convection, restricts the depth scale of convective motion, and aids the mantle in resisting geochemical homogenization.

We have used numerical experiments to study what controls the timescale of overturn and to look at the density structure after overturn. In particular, we are interested in whether the density structure is completely inverted with overturn or if lateral heterogeneities are created. Lateral heterogeneities could be important for understanding global scale asymmetries such as the crustal thickness dichotomy on Mars.

Models that treat the fractional crystallization of the magma ocean by determining bulk composition and phase assemblages *a priori* and calculate densities from thermochemical parameters predict densities that do not vary monotonically with depth. The overturn of overlapping density structures results in persistent lateral compositional heterogeneity with no lateral density variation (Figure 1).

Temperature-dependent and pressure-dependent viscosity have strong effects on the overturn time. With a stagnant lid, as seen in fluids with strongly-temperature dependent viscosity, two stages of overturn occur. The later stages of overturn are of significantly smaller scale. The timescales for the later stages of overturn are much longer than those predicted by the theorized Rayleigh-Taylor overturn of an unstable layer to a stable linear configuration.. For larger planets, pressure-dependence of viscosity strongly increases the viscosity of downwelling plumes and therefore slows the rate of overturn. In general, however, the timescales of the large-scale, first stage of overturn are rapid, except for cases with a very shallow magma ocean or very high mantle viscosities. This allows us to consider cases where the unstable crystallized magma ocean has almost fully overturned before thermal convection has begun.

We have used numerical experiments to study the convective behavior of a stably stratified viscous fluid cooled from above with strongly temperature-dependent viscosity. Strongly temperature dependent viscosity reduces the available thermal buoyancy and therefore increases the impact of compositional stratification. In our experiments, the fluid initially at a uniform temperature cools from above. The thermal boundary thickens by conduction until it becomes unstable. After the onset of convection, a convecting layer forms that cools and thickens with time (Figure 2a and 2b).

We looked at several aspects of convective behavior such as the delay of the onset time of convection, the penetration depth of the first downwelling, the thickening and cooling rate of the mixed layer, and the maximum depth of mixing. We have created simple scaling laws and parameterizations and have applied them to develop a broad understanding of planetary evolution. Scaling laws for the mixed layer thickening rate indicate that thickening occurs mainly by buoyant, rather than viscous, entrainment of the underlying stratified fluid (Figure 3). In several geologically realistic settings, our experiments predict a restricted depth

of stratification or mantle viscosities on the order of 10^{18} Pa s or less are required for convective instability. Therefore, compositional stratfication may not only be important in the early evolution of planets but also may alter their much later thermal evolution by affecting convection at the base of planetary lithospheres.

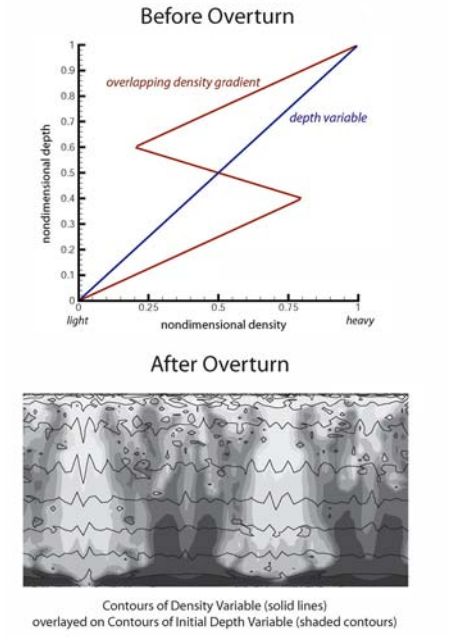

Figure 1: *Top* - Initial distribution of density as a function of depth in one of our numerical experiments with an unstable compositional stratification. Because the density does not monotonically decrease with depth, the initial depth of the fluid was also tracked in the experiment. *Bottom*- Distribution of density and initial depth after overturn. Different initial depths would correspond to different compositions (i.e. late-stage vs early-stage cumulates). Although overturn leads to an almost completely stable density stratification, the fluid is still compositonally heterogeneous.

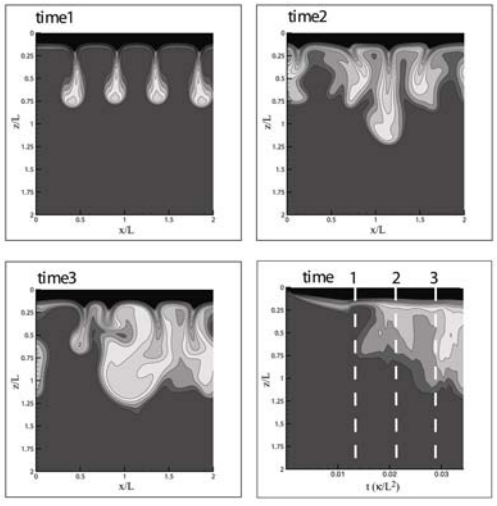

Figure 2a: Example of temperature fields in one of our numerical experiments with temperature-dependent viscosity and an initially stable compositional stratification. Temperature distribution is given at three times and the horizontally averaged temperature is given as a function of time. Vertical dashed lines show the horizontally averaged temperatures at the times of the three snapshots. After the onset of convection, a mixing, convecting layer thickens with time.

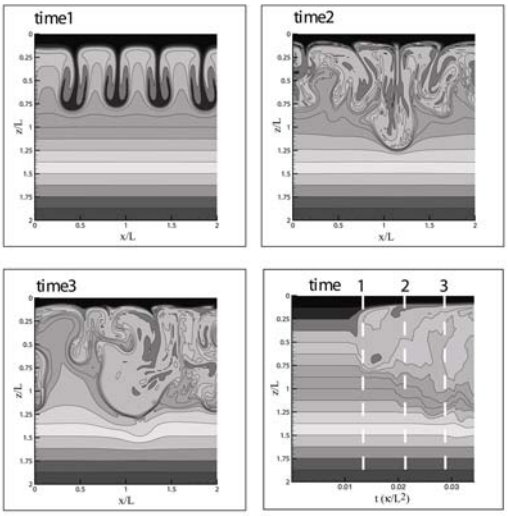

Figure 2b: Same as Figure 2a, except composition rather than temperature is plotted. The initial composition distribution is stable, with density increasing with depth.

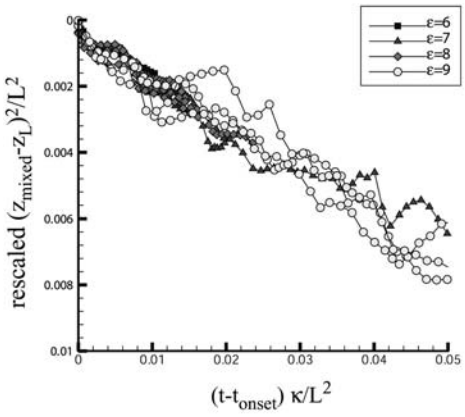

Figure 3: Rescaled mixed layer thickness as a function of non-dimensionalized time. The square of the non-dimensionalized rescaled mixed layer thickness increases linearly with depth as predicted by our scaling laws. ε is the parameter which controls the strength of the temperature-dependent viscosity, L is the depth of the experimental domain, and κ is thermal diffusivity.

The weak temperature gradient(WTG) approximation, in which the temperature tendency and advection terms are neglected in the temperature equation so that the equation reduces to a diagnostic balance between heating and vert ical motion, is applied to nonlinear shallow water model with the heating parameterized as a Newtonian relaxation on the layer thickness(the relevant temperature-like variable). Layer thickness variations are diagnosed from the ho rizontal flow using a balance constraint obtained from the divergence of the momentum equation. For this particula r heating parameterization, if all terms are retained in the equation, the balance condition transforms into a time-de pendent, diffustion type equation for the layer thickness. If the tendency term is dropped, a more standard elliptic b alance equation is obtained. In either case, the resulting thickness variations are then used in the heating parameteri zation, although they have been neglected in the thickness equation itself. The equations are solved numerically. A s tests of the solution algorithm, the solutions are used to reproduce earlier results using the same system in particu lar limits, namely a linear Gill-type problem and a nonlinear axisymmetric Hadley cell model. Then general nonlin ear solutions are obtained for forcing with two-dimensional structure and compared with the full shallow water sol utions in the parameters space(strength, shape, location of the heating and rayleigh damping rate). The comparison sheds light in understanding the relative roles of balanced and unbalanced motions in the tropics.